Supporting Information for

A Multi-Stimuli Responsive Ruthenium Complex for Catalytic Water Oxidation

Masanari Hirahara*[a], Hiroki Goto, Masayuki Yagi, and Yasushi Umemura [a]

Department of Applied Chemistry, School of Applied Science, National Defense Academy of Japan, Hashirimizu 1-10-20, Yokosuka, Kanagawa, 239-8686

Supporting Information

Contents

Experimental details S3
General considerations S3
Synthesis of C_2pyqu S6
Synthesis of *proximal*-[Ru(C_2tpy)(C_2pyqu)Cl]Cl S6
Synthesis of *proximal*-**1** S7
Synthesis of *distal*-**1** S7

NMR spectra S9
Figure S1—^{1}H NMR spectrum of C_2pq S9
Figure S2—^{13}C{^{1}H} NMR spectrum of C_2pq S9
Figure S3—^{1}H/^{1}H COSY NMR spectrum of C_2pq S10
Figure S4—^{1}H/^{13}C HSQC NMR spectrum of C_2pq S10
Figure S5—^{1}H/^{13}C HMBC NMR spectrum of C_2pq S10
Figure S6—^{1}H NMR spectrum of *proximal*-[Ru(C_2tpy)(C_2pq)Cl]Cl S11
Figure S7—^{13}C{^{1}H} NMR spectrum of *proximal*-[Ru(C_2tpy)(C_2pq)Cl]Cl S11
Figure S8—^{1}H/^{1}H COSY NMR spectrum of *proximal*-[Ru(C_2tpy)(C_2pq)Cl]Cl S12
Figure S9—^{1}H/^{13}C HSQC NMR spectrum of *proximal*-[Ru(C_2tpy)(C_2pq)Cl]Cl S12
Figure S10—^{1}H/^{13}C HMBC NMR spectrum of *proximal*-[Ru(C_2tpy)(C_2pq)Cl]Cl S12
Figure S11—^{1}H NMR spectrum of *proximal*-**1** S13
Figure S12—^{13}C{^{1}H} NMR spectrum of *proximal*-**1** S13
Figure S13—^{1}H/^{1}H COSY NMR spectrum of *proximal*-**1** S14
Figure S14—^{1}H/^{13}C HSQC NMR spectrum of *proximal*-**1** S14
Figure S15—^{1}H/^{13}C HMBC NMR spectrum of *proximal*-**1** S15
Figure S16—^{1}H NMR spectrum of *distal*-**1** S16
Figure S17—^{13}C{^{1}H} NMR spectrum of *distal*-**1** S16
Figure S18—^{1}H/^{1}H COSY NMR spectrum of *distal*-**1** S17

Figure S19—$^{1}H/^{13}C$ HSQC NMR spectrum of *distal*-**1** S17
Figure S20—$^{1}H/^{13}C$ HMBC NMR spectrum of *distal*-**1** S17

ESI-MS spectra
Figure S21—ESI-MS spectrum of *proximal*-[Ru(C_2tpy)(C_2pyqu)Cl]Cl S18
Figure S22—ESI-MS spectrum of *proximal*-**1** S18
Figure S23—ESI-MS spectrum of *distal*-**1** S19

Absorption spectra
Figure S24—Absorption spectra of *proximal*- and *distal*-**1** S20
Figure S25—Absorption spectra of *proximal*-**1** during titration experiments S20
Figure S26—Absorption spectra of *distal*-**1** during titration experiments S21

Additional figures for photo- and thermal-isomerizations
Figure S27—Excitation wavelength dependency of photoisomerization S22
Figure S28—Thermal isomerization of distal-1 at room temperature S23
Figure S29—Eyring plots for thermal isomerization reactions S24
Figure S30—van't Hoff plots for thermal isomerization reactions S24
Table S1— Summary of photoisomerization and thermal isomerization parameters S25

Additional figures for water oxidation experiments
Figure S31—Catalytic O_2 evolution measured with a Clark electrode S26
Figure S32—Plots of initial rate of O_2 evolution vs the amounts of complexes S26
Figure S33— Catalytic O_2 evolution measured with gas chromatography S27

Electrochemical measurements
Figure S34—Cyclic voltammograms of *proximal*- and *distal*-**1** S28
Figure S35—Cyclic voltammograms of *proximal*- and *distal*-**1** S28

Crystallographic information
Table S2—Crystal and Refinement Data for *proximal*- and *distal*-**1** S29
Table S3—Summary of bond lengths and angles or *proximal*- and *distal*-**1** S30

DFT calculations
Figure S36—Optimized structures of *proximal*- and *distal*-**1** S31
Figure S37—Energy diagrams for water nucleophilic attack S32
Figure S38—LUMOs of *proximal*- and *distal*-[Ru(C_2tpy)(C_2pq)O]$^{3+}$. S33
Cartesian coordinates and energies S34

References S42

Experimental Details

General considerations

Materials.

4'-ethoxy-2,2';6',2"-terpyridine (C_2tpy),[1] Ru(C_2tpy)Cl_3,[2] and 2-(2'-(6'-chloro)-pyridyl)quinoline[3] were prepared as previously described. Silica-gel column chromatography was performed using silica gel 60 (Kanto Chemical Co., Inc., 100-210 μm). Triflic acid was distilled under reduced pressure at 70 ºC, and then diluted to 1 M with distilled water right after the distillation. 2,2,2-trifluoroethanol was dried over with 4Å molecular sieves, and then distilled under nitrogen. All other reagents were purchased and used without further purification.

Measurements

^{1}H NMR spectra were recorded on a JEOL 500 MHz spectrometer. ^{1}H NMR spectra were referenced using tetramethylsilane in organic solvents or sodium 3-(trimethylsilyl)propionate-2,2,3,3-d_4 in D_2O as internal standard reagents. UV visible absorption spectra were measured in a quartz cell with 1 cm of a light path length using a photodiode array spectrometer (Hitachi U-3310). For the determination of quantum yield of photoisomerization of *proximal*-**1** or *distal*-**1**, the ruthenium complex was dissolved in CD_3OD (20%) and D_2O (80%) and transferred to an NMR tube, where the concentration of the complex and volume of the sample solution were 2 mM and 500 μL, respectively. The sidewall of the NMR tube was irradiated monochromic light (λ = 509 ± 1.5 nm, 1.6 mW cm^{-2}) at room temperature. The internal quantum yields for photosubstitution were given from the

$$\Phi = \frac{hcN_A k n_{int}}{p\lambda A(1-T)}$$

where k, n_{int}, h, p, λ, c, N_A, T and A are the initial rate constant for photosubstitution, initial amount of ruthenium complexes (1 × 10^{-6} mol), Plank's constant, photon flux (1.6 mW cm^{-2}), wavelength (5.09 × 10^{-7} m), the speed of light, Avogadro's number, the transmittance, and the irradiated area (1.2 cm^2), respectively. The transmittance of light can be regarded as zero because of large extinction coefficients of complexes at the wavelength (~9 x 10^3 M^{-1} cm^{-1}) and high concentration of sample (2 mM). The initial rate constants were determined from the slope of concentration change and irradiation time. NMR spectra

were processed with MNova software. Electrospray ionization mass spectra (ESI MS) were measured with a Waters/Micromass, ZQ 4000 spectrometer. The conditions were as follows: complex concentration, 5 − 40 μM in methanol; cone voltage, 20 V; capillary voltage, 3.5 kV. X-ray diffraction data were recorded using a Bruker APEXII CCD area detector diffractometer; the detector was positioned at a distance of 6.0 cm from the crystal and monochromated Mo Kα radiation (λ = 0.71073 Å) from a rotating anode with a mirror focusing apparatus operated at 1.2 kW (50 kV, 24 mA) was used. A sample crystal was mounted on a glass fiber for X-ray diffraction measurements. The structures were solved by direct methods and expanded using Fourier techniques. The non-hydrogen atoms were refined anisotropically. Hydrogen atoms on bidentate and tridentate ligands were included but not refined. The final cycle of full-matrix least-squares refinement was based on the observed reflections [$I > 2.00\ \sigma(I)$] and variable parameters, and converged with unweighted and weighted agreement factors R and R_w. The crystal structure was refined with Olex2 software and ORTEP views were plotted with ORTEP3. The electrochemical measurement was performed in a conventional single-compartment cell equipped with a glassy carbon electrode (e□ective area, 0.071 cm^2) as an working electrode, a saturated calomel electrode (SCE) as an reference electrode, and a platinum wire counter electrode at 25°C using an electrochemical analyzer (Hokuto Denko, HZ-3000). The glassy carbon working electrode was polished with polycrystalline diamonds (Struers, DP-Paste P, 1/4 μ m) and rinsed with water and acetone prior to use.

Water oxidation experiments

To a 20 mL vial equipped with a rubber septum were added ruthenium complexes, 20 μL of 2,2,2-trifluoroethanol, and then distilled water (1.5 ml). To the other vial equipped with a rubber septum and a magnetic stir bar were added ceric ammonium nitrate (0.75 mmol) and 0.1 M triflic acid (pH = 1.0, 13.5 ml). The two vials were connected with Teflon tube and then bubbled with argon gas for 30 minutes prior to the experiments. After the bubbling, the solution of the catalyst was transferred to the vial containing Ce^{IV} solution via a Teflon tube with argon pressure. The evolved oxygen gas in the headspace was collected using a microsyringe (Ito Seisakusho, MS-R100). The sample gas was analyzed on a gas chromatograph (Shimadzu, GC-2014) equipped with a molecular sieve 5 Å column using argon carrier gas (flow rate is 25 mL min^{-1}) at 40° C and a TCD detector. The chromatogram was analyzed with Chromatopac (Shimadzu, C-R8A). For the measurement of oxygen gas in liquid phase, Clark type oxygen electrode (Hansatech Instruments, Oxygraph OXYG1 and DW1/AD unit) was used. For the oxygen evolution after light irradiation, the bottom of the vial containing ruthenium complex in water and trifluoroethanol was irradiated with halogen lamp (λ > 340 nm) for 3h at room temperature.

DFT calculations

DFT calculations were performed using the Gaussian 16 package of programs.[4] Molecular structures were fully optimized using the B3LYP or UB3LYP method, which uses the hybrid Becke's three-parameter exchange functional[5] with the correlation energy functional of Lee, Yang, and Parr.[6] Calculations were performed using the standard double-ζ-type LanL2DZ basis set for Ru and 6-31G(d) for non-metal atoms. Molecular orbitals were visualized GaussView 6. The percentage contribution of groups to the molecular orbitals were calculated using GasussSum 3.0.[7]

Syntheses.

2-[2'-(6'-ethoxy)-pyridyl]quinoline (C_2pq): To a 300 mL round bottom flask equipped with a stir bar were added 2-[2'-(6'-chloro)-pyridyl]quinoline (540 mg, 2.24 mmol), NaOH (8 g, 0.2 mol), ethanol (100 mL). The reaction mixture was refluxed for 24 h, allowed to cool at room temperature, and evaporated to *ca.* 20 mL. An excess amount of water (100 mL) was added to the ethanol solution. The yellow precipitate was collected by filtration and dried under vacuum. The crude product was recrystallized from a mixed solution of water and ethanol. The colorless precipitate was collected and dried under vacuum. Yield 474 mg (84.5 %). Anal. calcd. for $H_{14}C_{16}N_2O$: C, 76.78; H, 5.64; N, 11.19. Found: C, 76.80; H,5.57, N, 11.43. ^{1}H NMR (500.16 MHz, $CDCl_3$) δ 8.55 (d, J = 8.6 Hz, 1H), 8.37 – 8.12 (m, 3H), 7.85 (d, J = 8.2 Hz, 1H), 7.81 – 7.68 (m, 2H), 7.62 – 7.50 (m, 1H), 6.82 (d, J = 8.2 Hz, 1H), 4.55 (q, J = 7.1 Hz, 2H), 1.49 (t, J = 7.1 Hz, 3H). ^{13}C NMR (125.75 MHz, $CDCl_3$) δ 163.4, 156.2, 153.3, 147.6, 139.6, 137.0, 129.8, 129.6, 128.3, 127.7, 126.8, 119.2, 114.7, 111.74, 77.37, 77.12, 61.8, 14.8.

***Proximal*-[Ru(C_2tpy)(C_2pq)Cl]Cl:** To a 200 mL round bottom flask equipped with a stir bar were added Ru(C_2tpy)Cl_3 (199 mg, 0.41 mmol), C_2pq (98 mg, 0.39 mmol), triethylamine (1.0 mL), LiCl (300 mg), and 1-propanol (50 mL). The reaction mixture was refluxed under nitrogen for a week followed by evaporation to dryness under reduced pressure at 45°C. The solid was suspended in chloroform and filtered through Celite. The filtrate was concentrated to ~10 mL by a rotary evaporator and an excess amount of ether (~100 mL) was added. The crude product was filtered and washed with 3 M HCl and ether. The solid was purified silica gel chromatography. The dark brown impurities were eluted with chloroform. The purple colored product was eluted with 4% methanol in chloroform. Yield 107 mg (33 %). Anal. calcd. for *proximal*-[Ru(C_2tpy)(C_2pq)Cl]Cl·3HCl·H_2O, $H_{34}C_{33}N_5O_3Cl_3Ru_1$: C, 47.93; H, 4.14; N, 8.47. Found: C, 47.84; H, 4.18, N, 8.67. ^{1}H NMR (500.16 MHz, $CDCl_3$) 9.58 (d, J = 8.4 Hz, 1H), 8.56 (s broad, 2H), 8.35 – 8.00 (m, 4H), 7.97 – 7.50 (m, 9H), 7.12 (s broad, 2H), 6.54 (s broad, 1H), 4.42 (s broad, 2H), 3.67 (s broad, 2H), 1.54 (s broad, 3H), 0.79 (s broad, 3H). Peaks were significantly broadened, which was also observed in higher temperature (45°C). ^{13}C NMR (125.75 MHz, $CDCl_3$) δ 169.7, 165.4, 160.2, 159.3, 158.9, 158.2, 153.0, 151.4, 139.9, 137.8, 137.0, 131.2, 131.1, 129.3, 129.0, 128.4, 127.0, 123.8, 119.9, 119.1, 109.8, 107.8, 66.9, 66.4, 14.8, 14.1. ESI MS of *proximal*-[Ru(C_2tpy)(C_2pyqu)Cl]Cl (solvent: methanol) m/z (calcd): 314.62 (314.57, $[M - H_2O - 2Cl]^{2+}$)).

***P*roximal-[1](OTf)$_2$**: To a 50 mL round bottom flask were added *proximal*-[Ru(C_2tpy)(C_2pq)Cl]Cl (50 mg, 60 μmol), silver triflate (30 mg, 117 μmol), acetone (3 mL), and water (10 mL). The reaction mixture was refluxed in the dark for 2h and filtered through Celite. Lithium triflate (300 mg) was added to the filtrate and the red-colored solution was evaporated to *ca.* 3 mL under reduced pressure at 45°C. The dark-red solid was collected on frit, washed with water (~0.5 mL), and dried in vacuum. Yield: 36 mg (62 %). Anal. calcd. for *proximal*-[**1**](OTf)$_2$·H_2O, $H_{33}C_{35}N_5O_{10}F_6S_2Ru$: C, 43.66; H, 3.45; N, 7.27. Found: C, 43.63; H, 3.22, N, 7.45. ^{1}H NMR (500.16 MHz, 20% CD_3OD and 80% D_2O) δ 8.58 (d, *J* = 8.8 Hz, 1H, quinoline-*H*), 8.53 – 8.49 (m, 1H, quinoline-*H*), 8.47 (d, *J* = 8.8 Hz, 1H, quinoline-*H*) 8.23 (d, *J* = 8.1 Hz, 2H, tpy-*H*), 8.13 – 8.07 (m, 1H, quinoline-*H*), 8.04 – 7.94 (m, 3H, tpy-*H* and pyridine-*H*), 7.76 (td, *J* = 7.9, 1.5 Hz, 2H, tpy-*H*), 7.68 – 7.64 (m, 2H, quinoline-*H*), 7.60 – 7.52 (m, 3H, tpy-*H* and pyridine-*H*), 7.09 (ddd, J = 7.3, 5.6, 1.3 Hz, 2H, tpy-*H*), 6.43 (d, *J* = 8.5 Hz, 1H, pyridine-*H*), 4.36 (q, *J* = 7.0 Hz, 2H, tpy-CH_2), 3.53 (q, *J* = 7.0 Hz, 2H, pyqu-CH_2), 1.40 (t, *J* = 7.0 Hz, 3H, tpy-CH_3), 0.61 (t, *J* = 7.0 Hz, 3H, pyqu-CH_3). ^{13}C NMR (125.75 MHz, 20% CD_3OD and 80% D_2O) δ 169.8 (pyridine-*C*), 166.1 (tpy-*C*), 160.0 (tpy-*C*), 159.6 (tpy-*C*), 158.9 (pyridine-*C*), 158.4 (quinoline-*C*), 153.6 (tpy-*C*), 150.6 (quinoline-*C*), 139.1 (pyridine-*C*), 137.9 (tpy-*C*), 137.7 (quinoline-*C*), 131.4 (quinoline-*C*), 129.2 (quinoline-*C*), 129.0 (quinoline-*C*), 128.8 (quinoline-*C*), 127.3 (tpy-*C*), 127.1 (quinoline-*C*), 123.3 (tpy-*C*), 119.5 (quinoline-*C*), 118.2 (pyridine-*C*), 109.9 (tpy-*C*), 107.1 (pyridine-*C*), 65.9 (tpy-*C*H_2), 65.4 (pyqu-*C*H_2), 13.7 (tpy-*C*H_3), 12.7. (pyqu-*C*H_3). ^{1}H NMR spectrum of *proximal*-[**1**]Cl_2 where the sample was obtained by dissolving the *proximal*-[(C_2tpy)(C_2pyqu)Cl]Cl in D_2O showed same peaks as isolated *proximal*-[**1**](OTf)$_2$. ESI MS of *proximal*-[**1**](OTf)$_2$ (solvent: methanol) m/z (calcd): 314.67 (314.57, [M – H_2O – 2OTf]$^{2+}$)). UV-vis: λ/ nm (ε/ 10^3 mol^{-1} L cm^{-1}) in H_2O, 250 (38.6), 310 (37.2), 520 (9.6).

***Distal*-[1](OTf)$_2$**: To a 300 mL tall beaker were added *proximal*-[Ru(C_2tpy)(C_2pq)Cl]Cl (52 mg, 62 μmol), acetone (10 mL), and water (60 mL). The reddish colored solution was illuminated with halogen lamp (120 mW cm^{-2}) for overnight at room temperature. To a 200 mL round bottom flask were added the reaction mixture and lithium triflate (~2 g) and then the mixture was filtered through Celite. The filtrate was evaporated with rotary evaporator (25 °C, 41 mmHg) under illumination with halogen lamp for 2 days. During the evaporation, large crystals (~0.3 mm) of *distal*-**1** were selectively obtained and used for X-ray crystallography. Yield 29 mg (48 %). Anal. calcd. for *distal*-[**1**]·(OTf)$_2$·2H_2O, $H_{35}C_{35}N_5O_{11}F_6S_2Ru$: C, 42.86; H, 3.60; N, 7.14. Found: C, 42.64; H, 3.51, N, 7.17. ^{1}H NMR (500.16 MHz, 20% CD_3OD and 80% D_2O) δ 8.32 (d, *J* = 7.8 Hz, 1H, pyridine-*H*), 8.22 (t, *J* = 8.2 Hz, 1H,

pyridine-*H*), 8.17 (d, *J* = 8.2 Hz, 3H, tpy-*H* and quinoline-*H*), 8.01 (s, 2H, tpy-*H*), 7.94 (d, *J* = 8.7 Hz, 1H, quinoline-*H*), 7.84 (d, *J* = 5.5 Hz, 2H, tpy-*H*), 7.75 (t, *J* = 7.9 Hz, 2H, tpy-*H*), 7.54 (d, *J* = 8.0 Hz, 1H, quinoline-*H*), 7.40 (d, *J* = 8.5 Hz, 1H, pyridine-*H*), 7.21 (t, *J* = 7.3 Hz, 1H, quinoline-*H*), 7.17 (t, *J* = 6.8 Hz, 2H, tpy-*H*), 7.06 (t, *J* = 8.1 Hz, 1H, quinoline-*H*), 6.72 (d, *J* = 8.9 Hz, 1H, quinoline-*H*), 4.36 (q, *J* = 7.0 Hz, 4H, tpy-CH_2 and pyridine-CH_2), 1.40 (t, *J* = 6.9 Hz, 3H, -CH_3), 1.13 (t, *J* = 7.0 Hz, 3H, -CH_3). ^{13}C NMR (125.75 MHz, 20% CD_3OD and 80% D_2O) δ 169.2 (pyridine-*C*), 166.5 (tpy-*C*), 161.7 (quinoline- *C*), 159.7 tpy -*C*), 159.2 (tpy -*C*), 156.5 (pyridine-*C*), 153.8 (tpy-*C*), 151.5 (quinoline-*C*), 140.7 (pyridine-*C*), 138.1 (tpy-*C*), 136.8 (quinoline -*C*), 130.6 (quinoline -*C*), 129.1 (quinoline-*C*), 128.1 (quinoline-*C*), 127.9 (quinoline-*C*), 127.5 (tpy-*C*), 124.0 (quinoline-*C*), 123.7 (tpy-*C*), 119.3 (quinoline -*C*), 118.6 (pyridine-*C*), 110.6 (tpy-*C*), 109.1 (pyridine-*C*), 66.5 (-*C*H_2), 66.0 (-*C*H_2), 13.62 (-*C*H_3), 13.40 (-*C*H_3). ESI MS of *distal*-[**1**] $(OTf)_2$ (solvent: methanol) m/z (calcd): 314.61 (314.57, [M – H_2O – 2OTf]$^{2+}$)). UV-vis: λ/ nm (ε/ 10^3 mol^{-1} L cm^{-1}) in H_2O, 245 (37.9), 274 (28.3), 311 (38.6), 520 (9.4).

NMR spectra

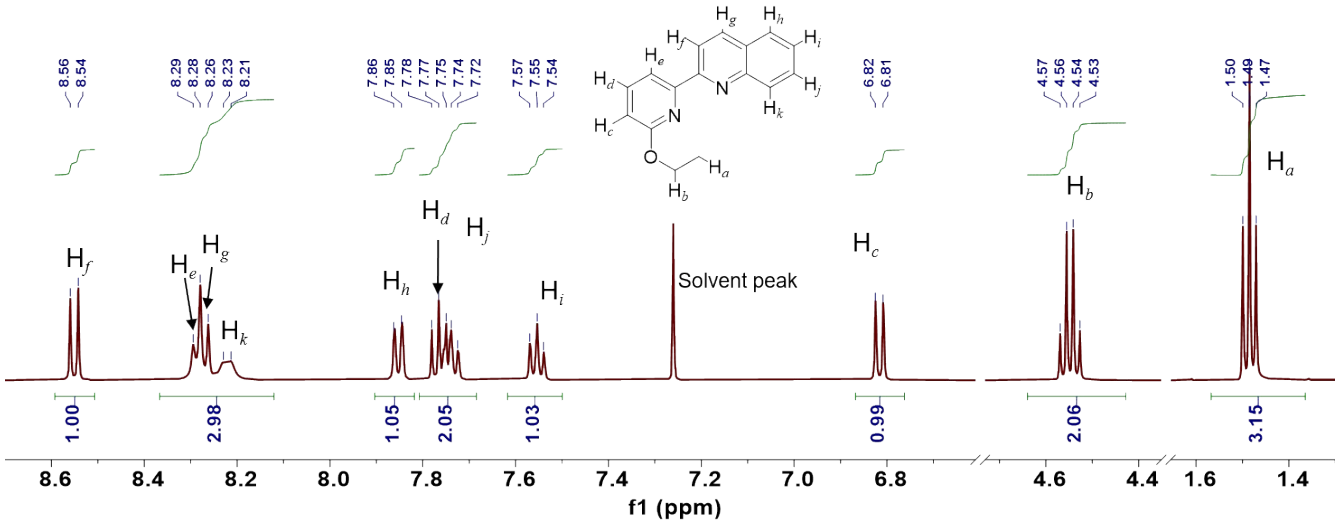

Figure S1. ^{1}H NMR Spectrum (500.16 MHz, $CDCl_3$, 23°C) of C_2pq.

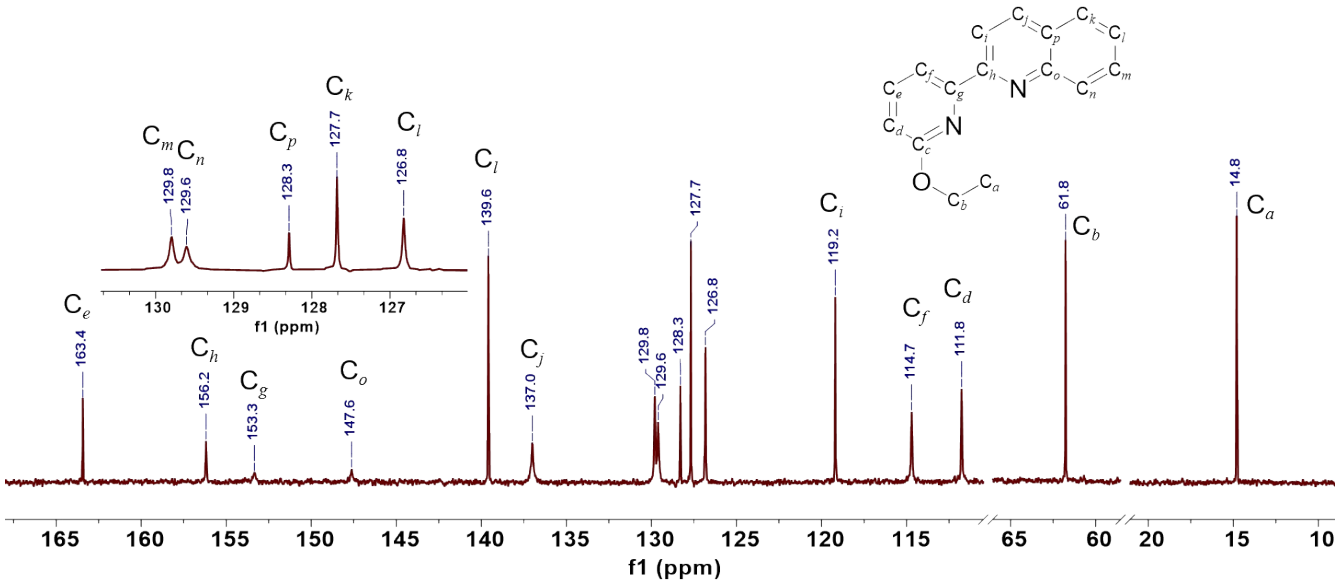

Figure S2. ^{13}C NMR Spectrum (125.75 MHz, $CDCl_3$, 23°C) of C_2pq.

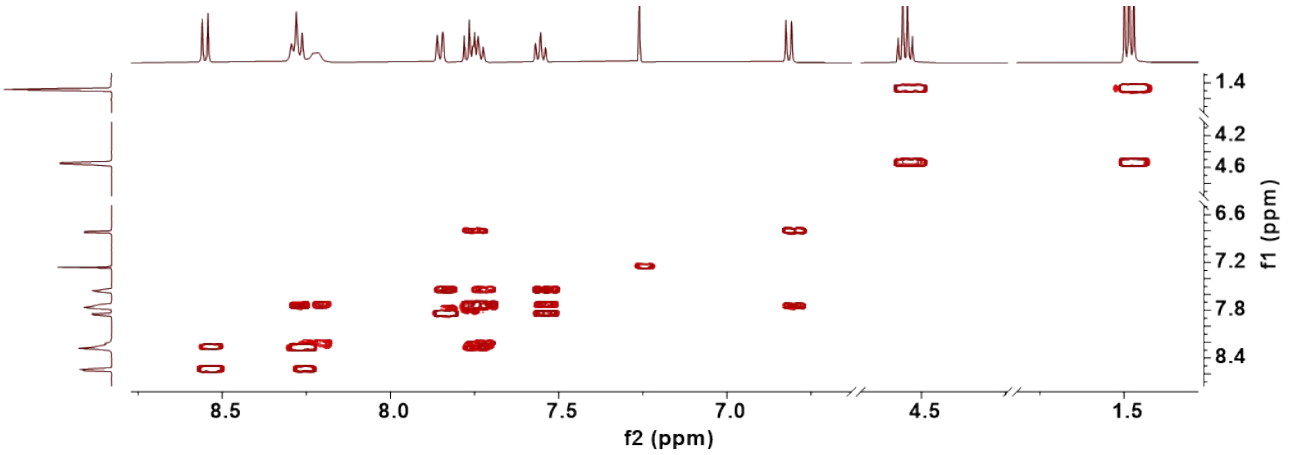

Figure S3. $^{1}H/^{1}H$ COSY Spectrum (500.16 MHz, $CDCl_3$, 23°C) of C_2pq.

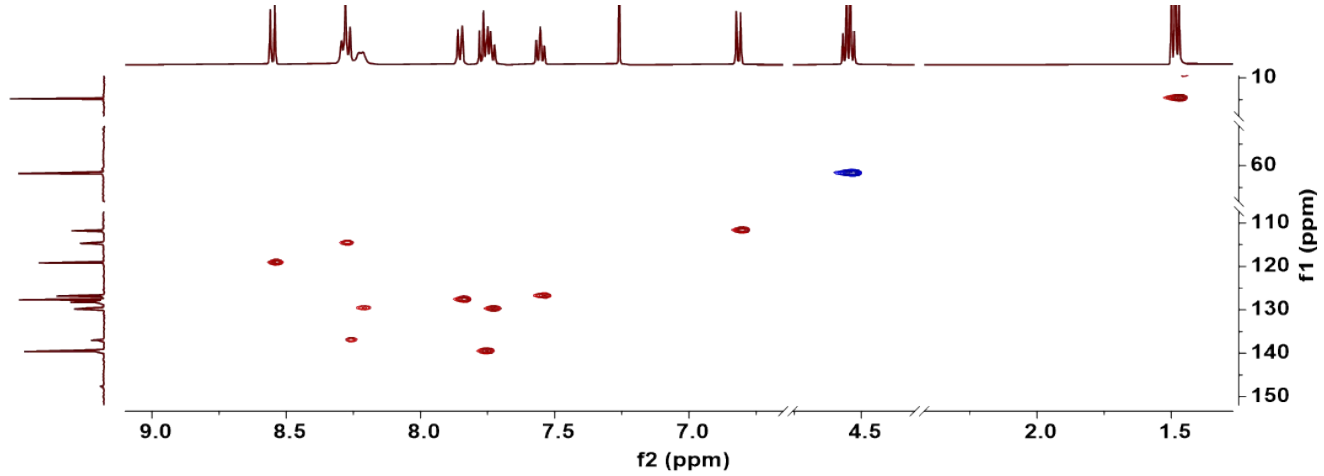

Figure S4. $^{1}H/^{13}C$ HSQC Spectrum (500.16/125.75 MHz, $CDCl_3$, 23°C) of C_2pq.

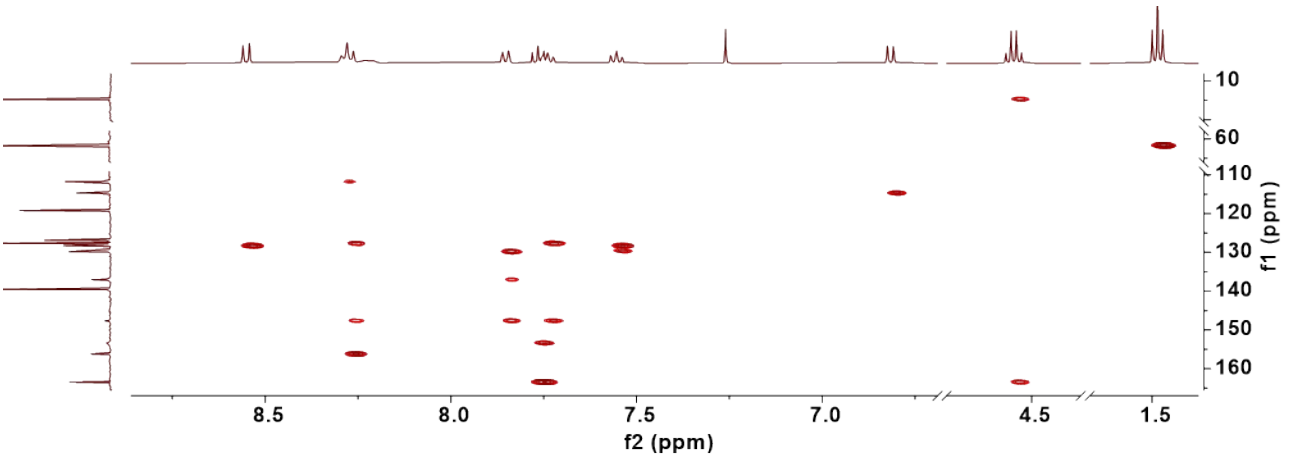

Figure S5. $^{1}H/^{13}C$ HMBC Spectrum (500.16/125.75 MHz, $CDCl_3$, 23°C) of C_2pq.

.

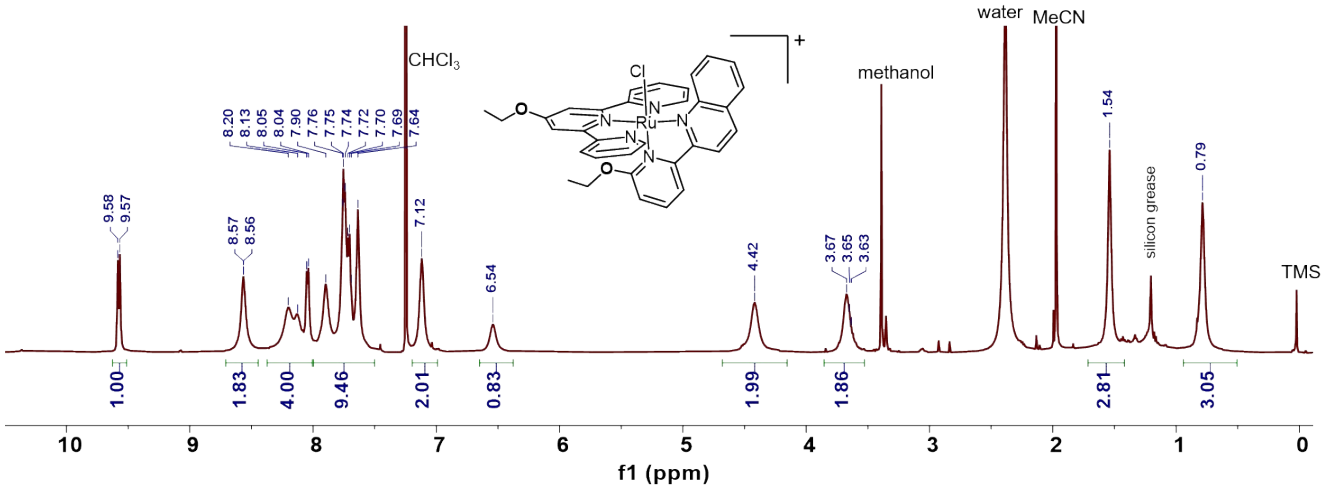

Figure S6. ^{1}H NMR Spectrum (500.16 MHz, $CDCl_3$, 23°C) of *proximal*-[(C_2tpy)(C_2pq)RuCl]Cl. Peaks were broadened even at 45°C.

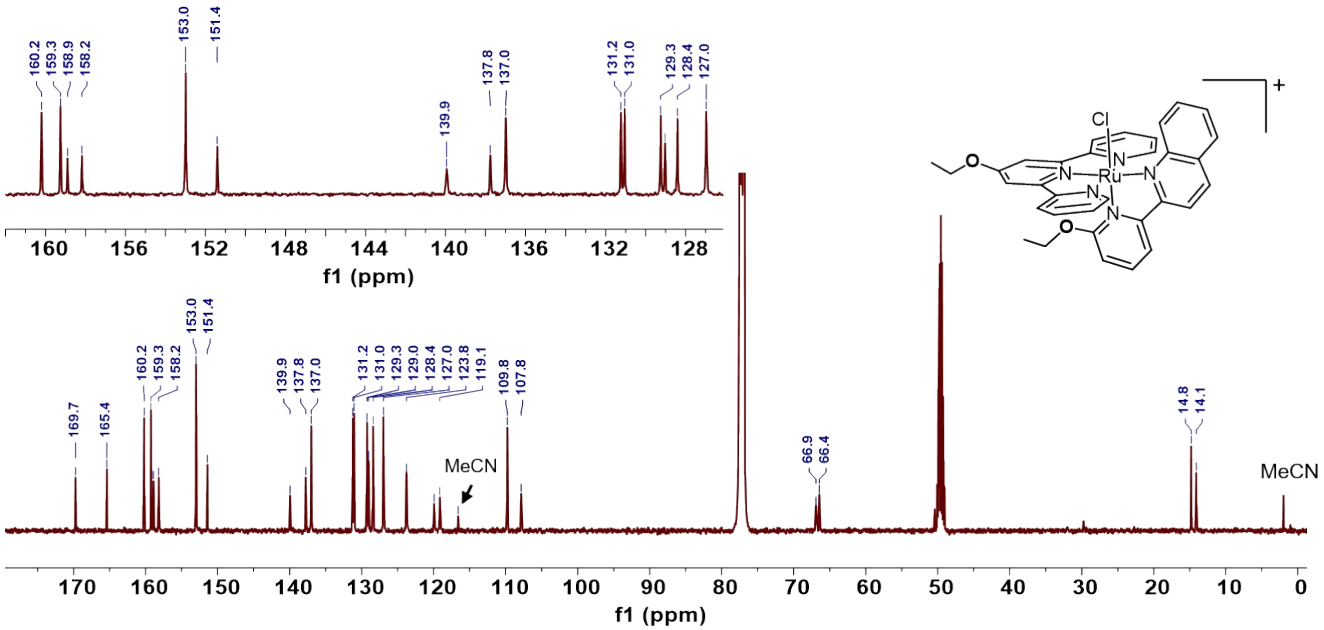

Figure S7. ^{13}C NMR Spectrum (125.75 MHz, $CDCl_3$, 23°C) of *proximal*-[(C_2tpy)(C_2pq)RuCl]Cl.

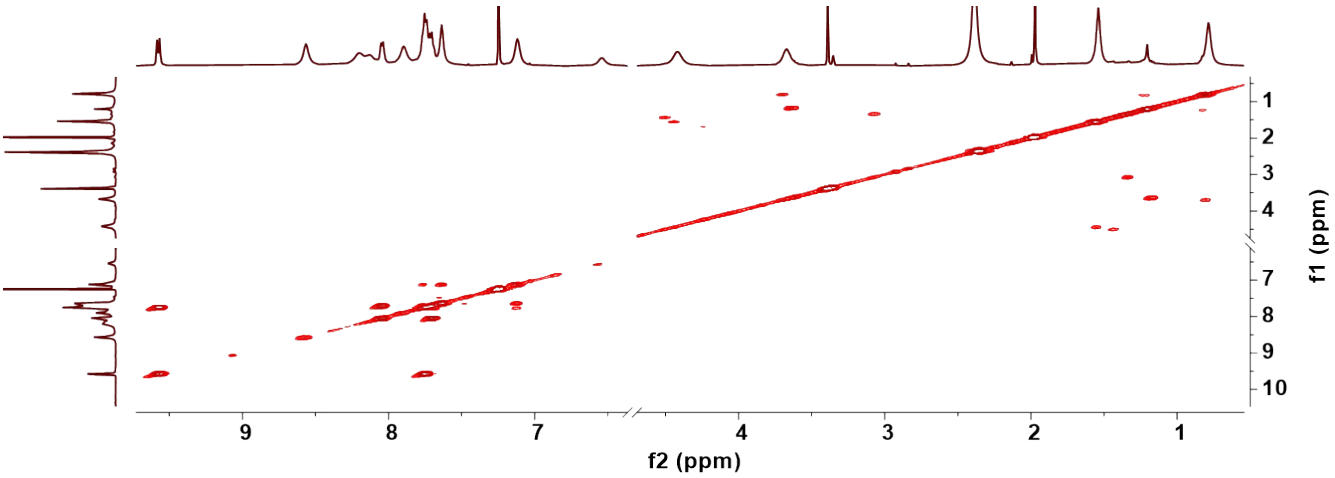

Figure S8. $^{1}H/^{1}H$ COSY Spectrum (500.16 MHz, $CDCl_3$, 23°C) of *proximal*-[(C_2tpy)(C_2pq)RuCl]Cl.

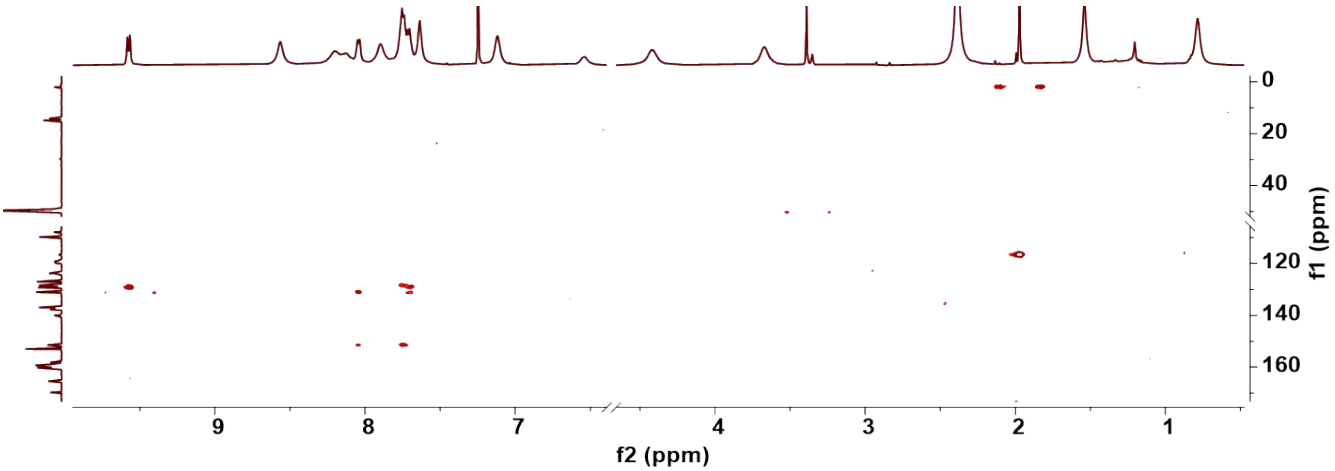

Figure S9. $^{1}H/^{13}C$ HSQC Spectrum (500.16/125.75 MHz, $CDCl_3$, 23°C) of *proximal*-[(C_2tpy)(C_2pq)RuCl]Cl.

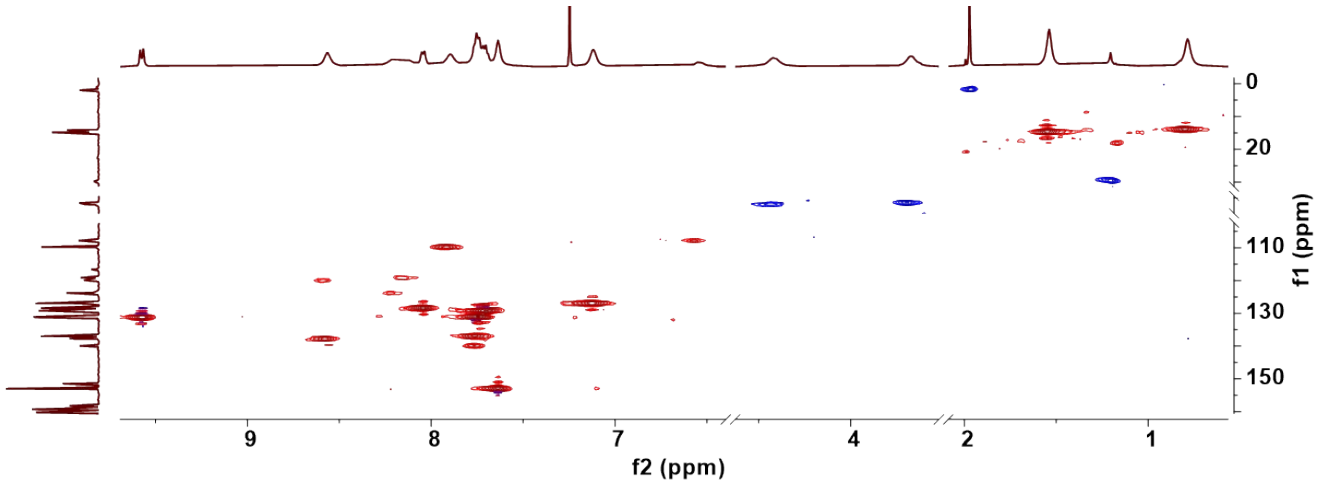

Figure S10. $^{1}H/^{13}C$ HMBC Spectrum (500.16/125.75 MHz, $CDCl_3$, 23°C) of *proximal*-[(C_2tpy)(C_2pq)RuCl]Cl.

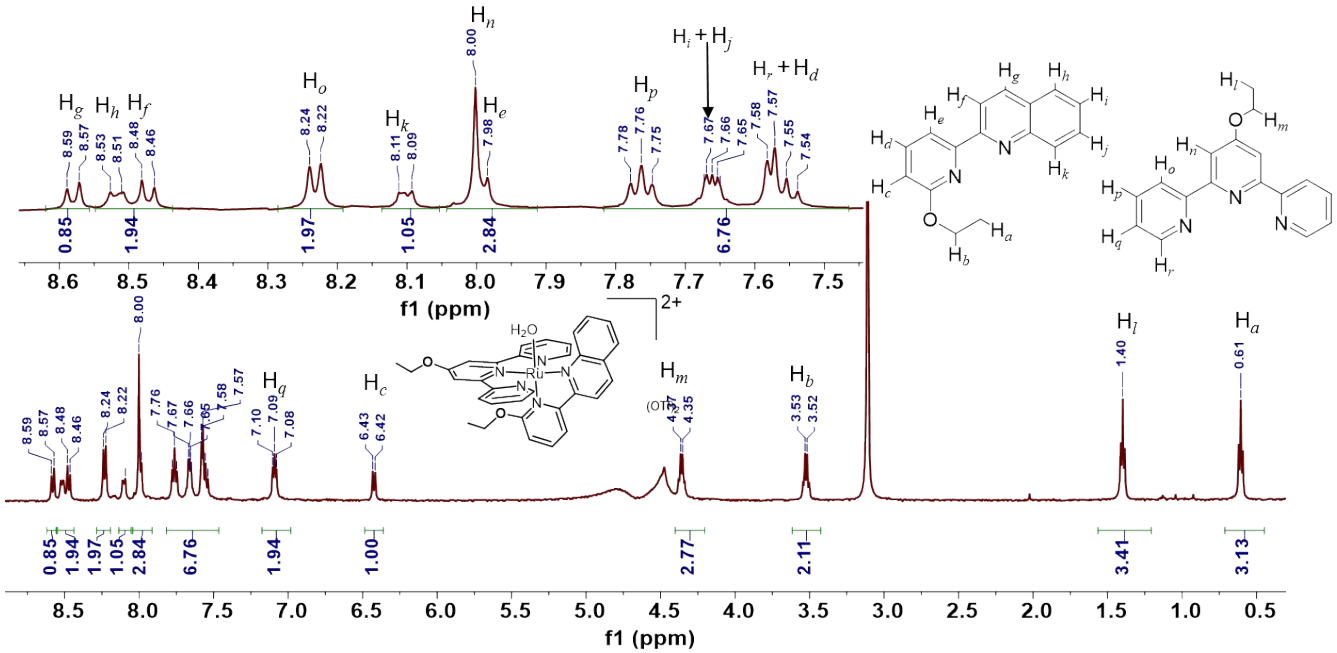

Figure S11. ^{1}H NMR Spectrum (500.16 MHz, 80% D_2O and 20% CD_3OD, 23°C) of *proximal*-[**1**](OTf)$_2$.

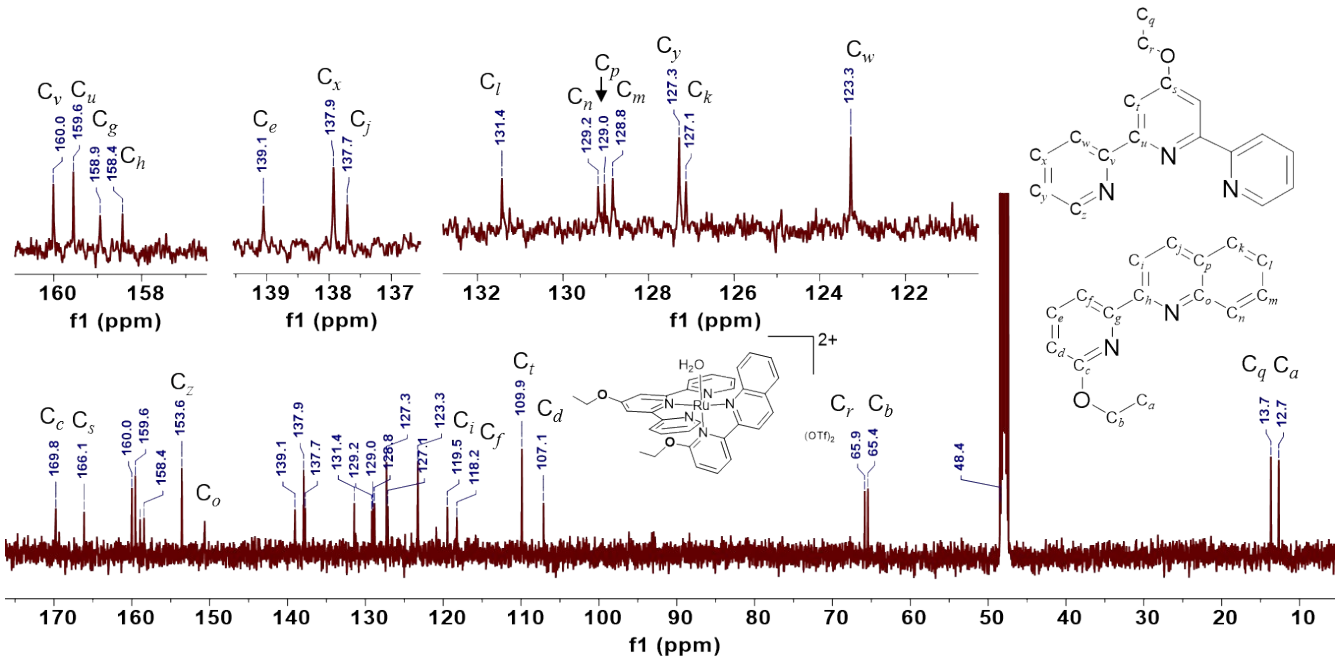

Figure S12. ^{13}C NMR Spectrum (125.75 MHz, 80% D_2O and 20% CD_3OD, 23°C) of *proximal*-[**1**](OTf)$_2$.

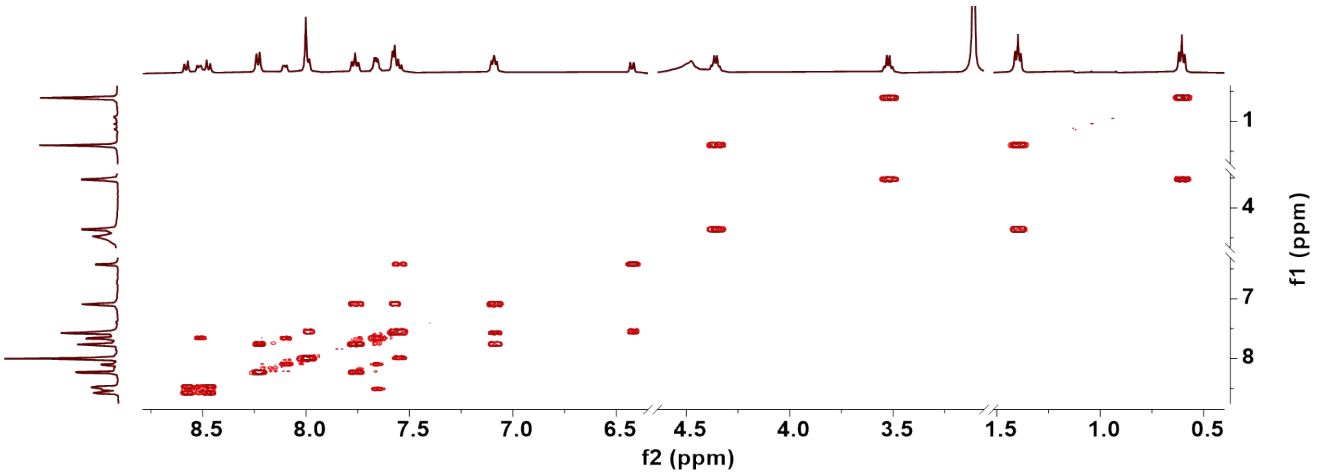

Figure S13. $^{1}H/^{1}H$ COSY Spectrum (500.16 MHz, 80% D_2O and 20% CD_3OD, 23°C) of *proximal*-[**1**](OTf)$_2$.

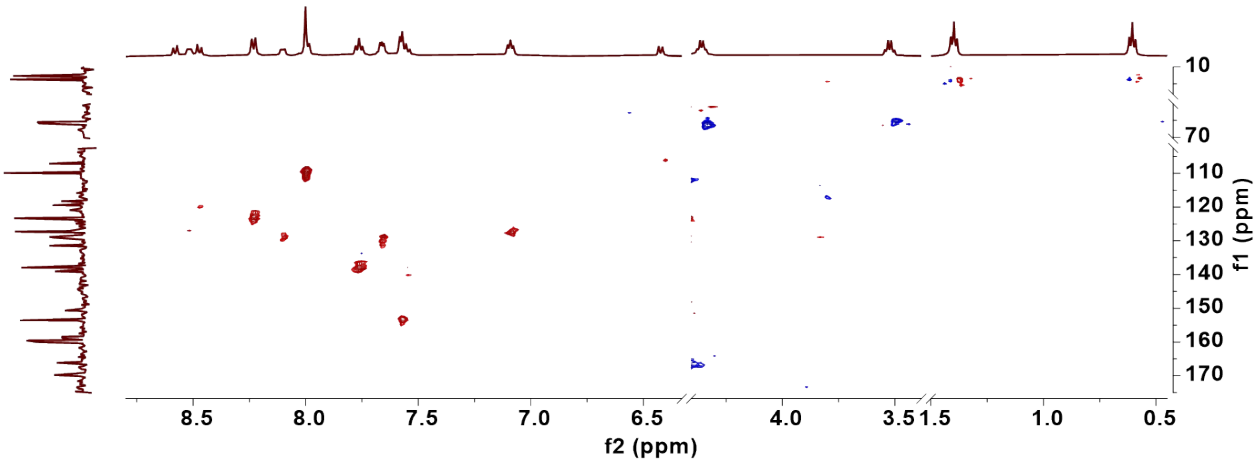

Figure S14. $^{1}H/^{13}C$ HSQC Spectrum (500.16/125.75 MHz, D_2O and 20% CD_3OD, 23°C) of *proximal*-[**1**](OTf)$_2$.

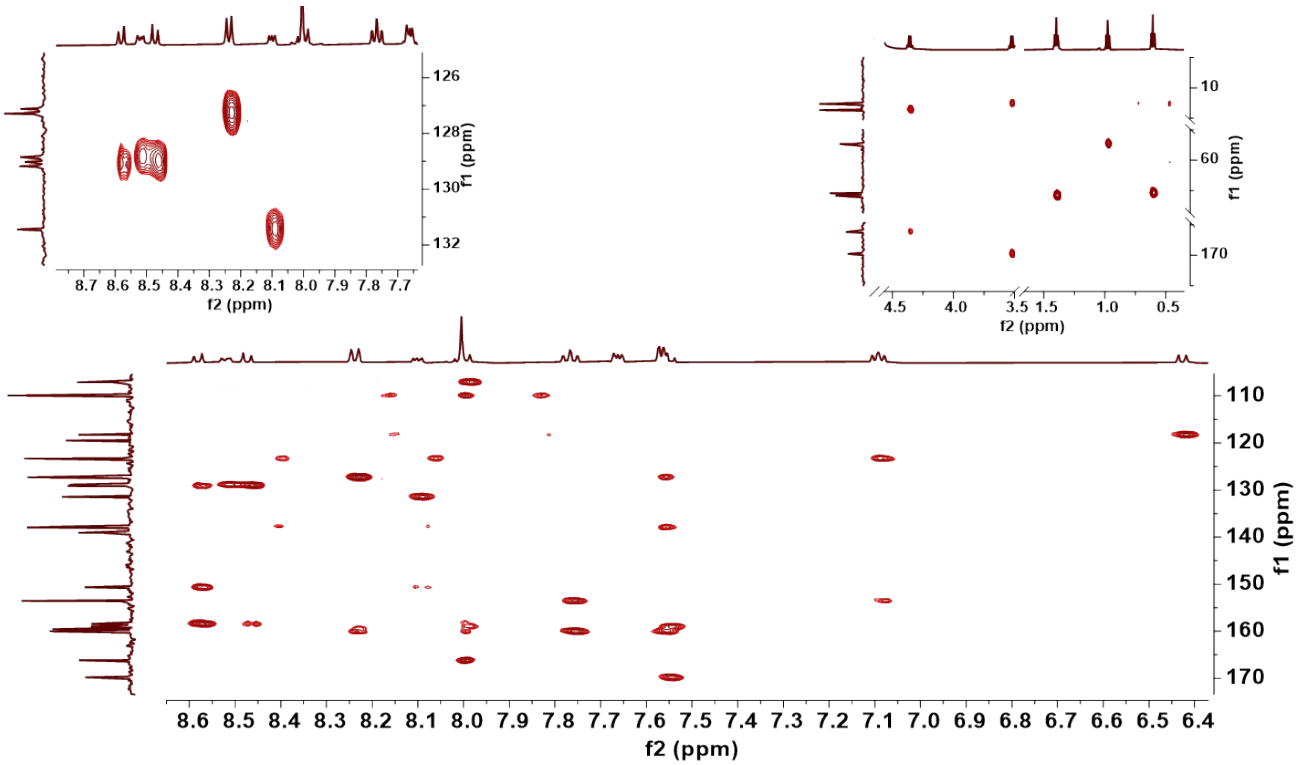

Figure S15. $^{1}H/^{13}C$ HMBC Spectrum (500.16/125.75 MHz, 80% D_2O and 20% CD_3OD, 23°C) of *proximal*-[**1**](OTf)$_2$.

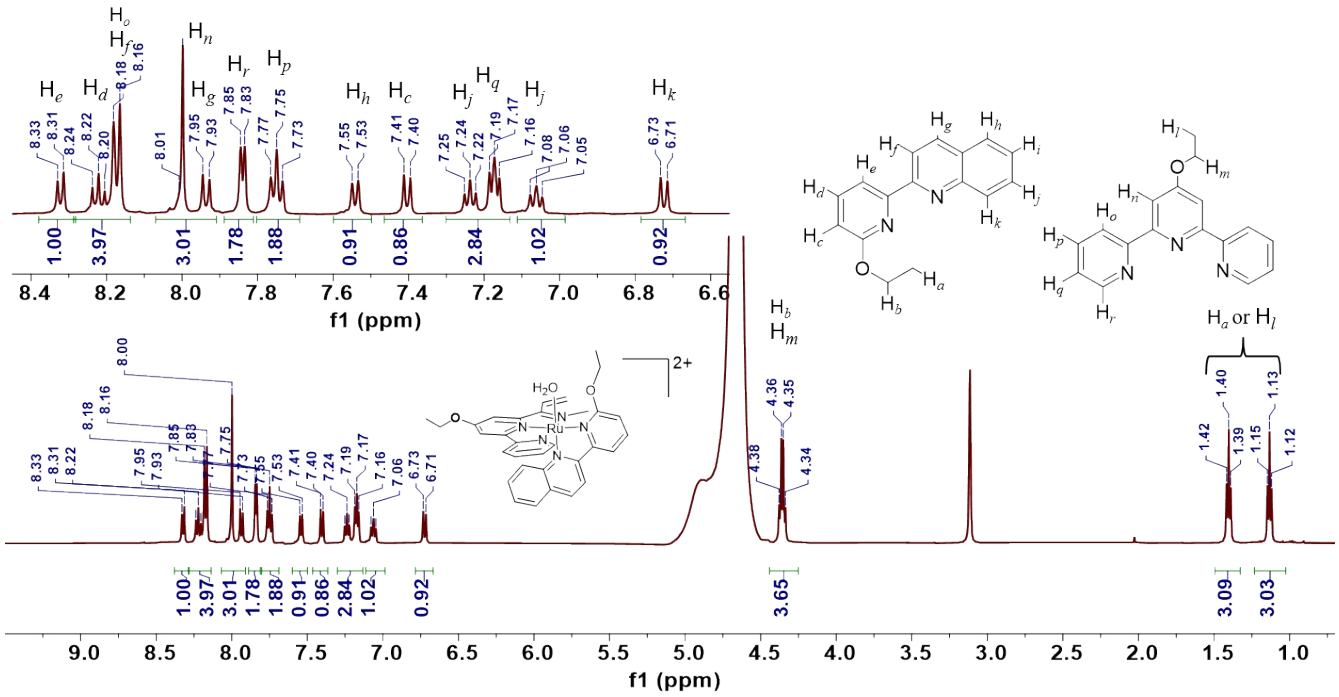

Figure S16. ^{1}H NMR Spectrum (500.16 MHz, 80% D_2O and 20% CD_3OD, 23°C) of *distal*-[**1**](OTf)$_2$.

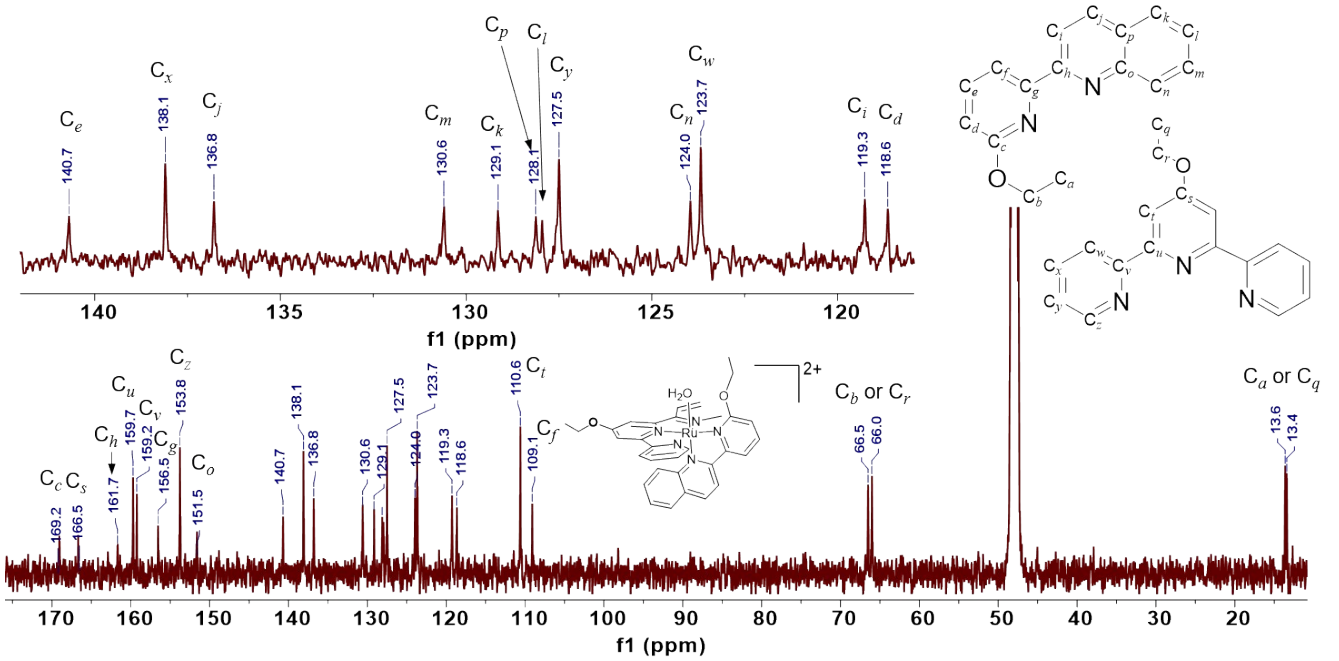

Figure S17. ^{13}C NMR Spectrum (125.75 MHz, 80% D_2O and 20% CD_3OD, 23°C) of *distal*-[**1**](OTf)$_2$.

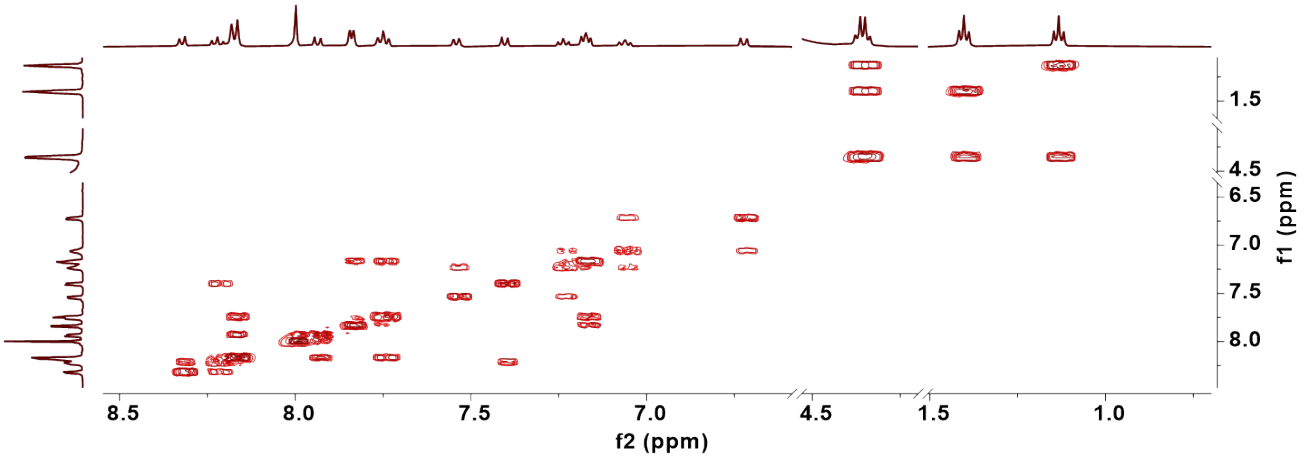

Figure S18. $^{1}H/^{1}H$ COSY Spectrum (500.16 MHz, 80% D_2O and 20% CD_3OD, 23°C) of *distal*-[**1**](OTf)$_2$.

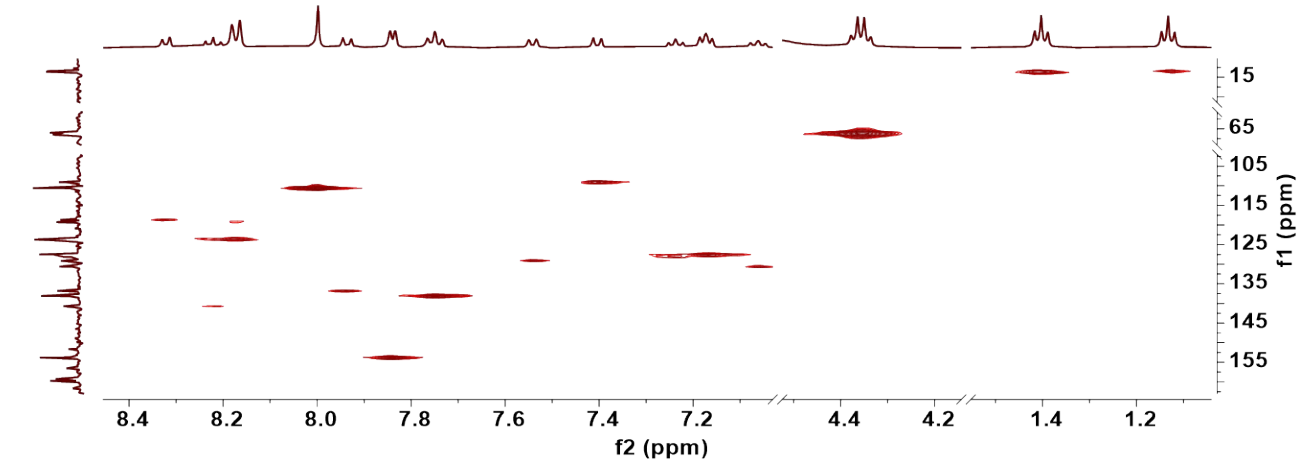

Figure S19. $^{1}H/^{13}C$ HSQC Spectrum (500.16/125.75 MHz, D_2O and 20% CD_3OD, 23°C) of *distal*-[**1**](OTf)$_2$.

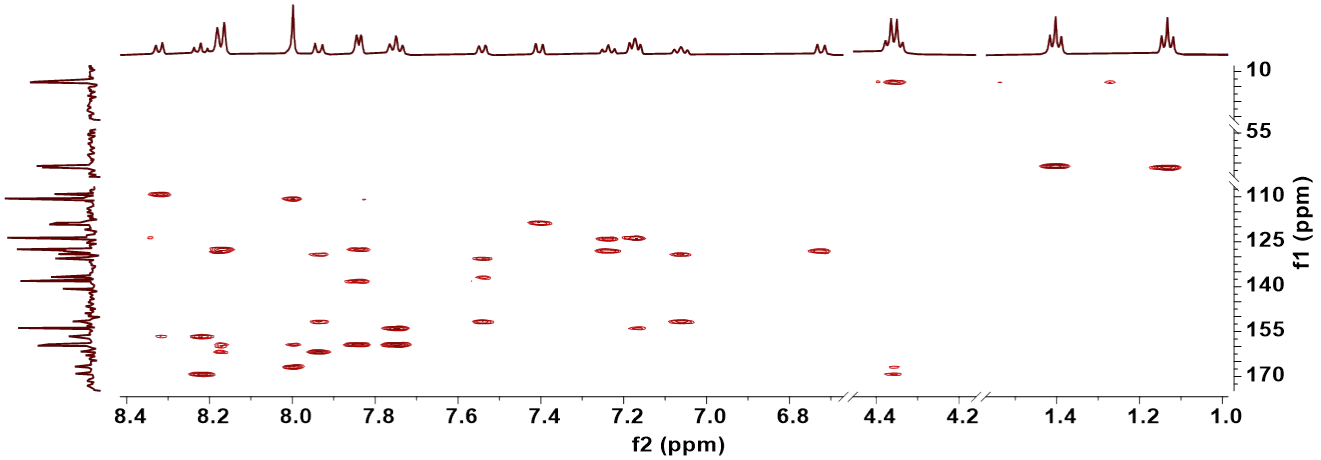

Figure S20. $^{1}H/^{13}C$ HMBC Spectrum (500.16/125.75 MHz, D_2O and 20% CD_3OD, 23°C) of *distal*-[**1**](OTf)$_2$.

ESI MS spectra

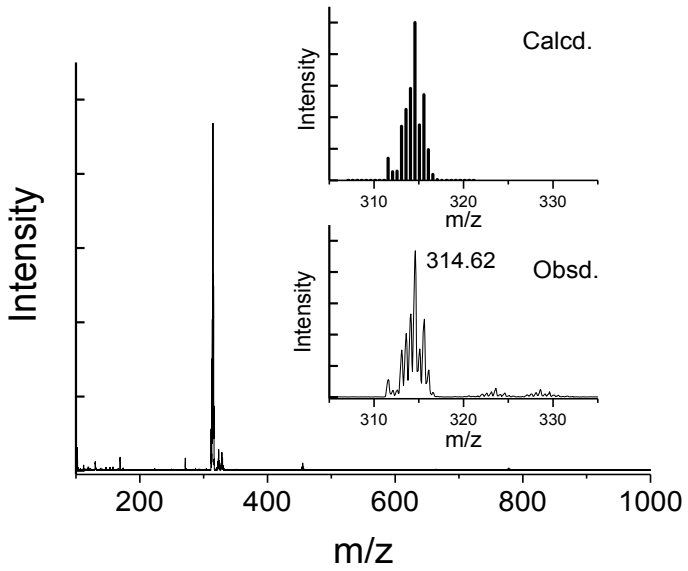

Figure S21. ESI MS spectrum of *proximal*-[Ru(C_2tpy)(C_2pyqu)Cl]Cl in CH_3OH. Inset shows isotopic distribution patterns of the observed and calculated peaks at 314.62 (*proximal*-[Ru(C_2tpy)(C_2pq)]$^{2+}$) m/z.

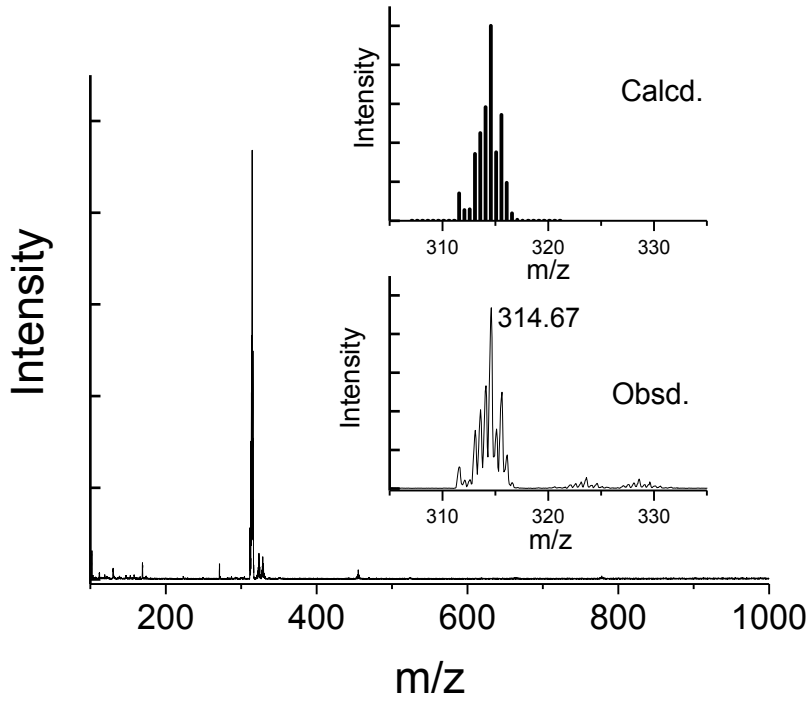

Figure S22. ESI MS spectrum of *proximal*-[**1**](OTf)$_2$ in CH_3OH. Inset shows isotopic distribution patterns of the observed and calculated peaks at 314.67 (*proximal*-[Ru(C_2tpy)(C_2pq)]$^{2+}$) m/z.

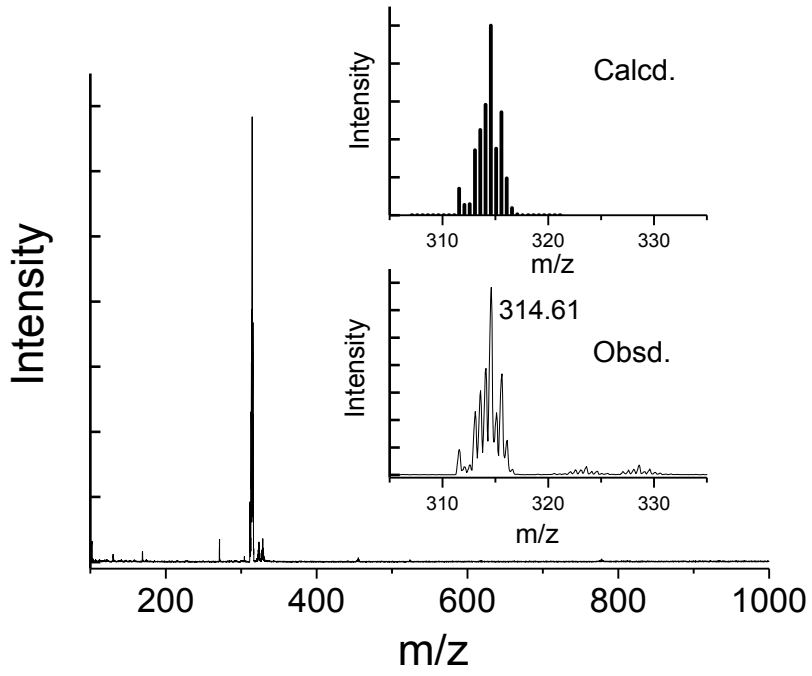

Figure S23. ESI MS spectrum of *distal*-[**1**](OTf)$_2$ in CH_3OH. Inset shows isotopic distribution patterns of the observed and calculated peaks at 314.61 (*distal*-[Ru(C_2tpy)(C_2pq)]$^{2+}$) m/z.

Absorption spectra

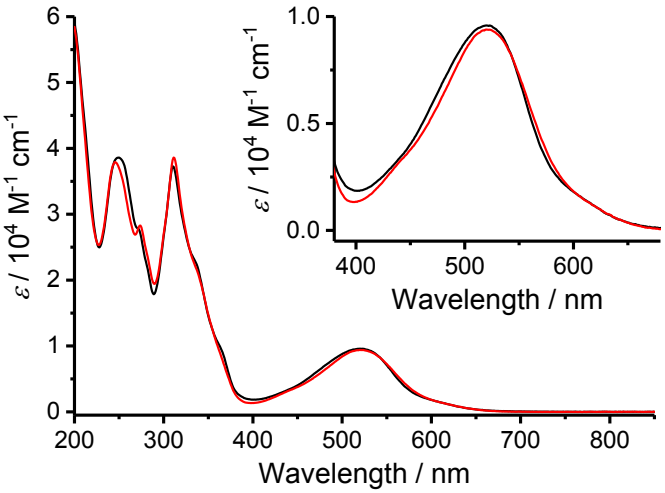

Figure S24. Absorption spectra of *proximal*-**1** (black) and *distal*-**1** (red) in water containig 0.2 % of methanol.

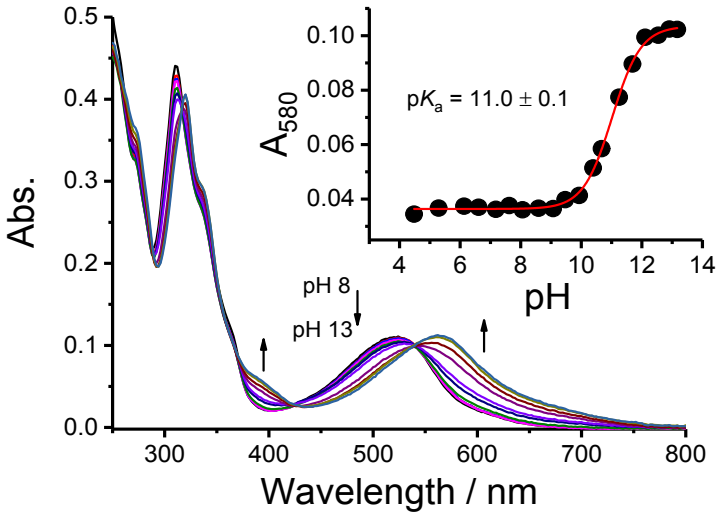

Figure S25. Absorption spectra of *proximal*-**1** during pH titration experiment in an aqueous buffer containing in boric acid (0.1 M), KH_2PO_4 (0.05 M), and citric acid (0.02 M).

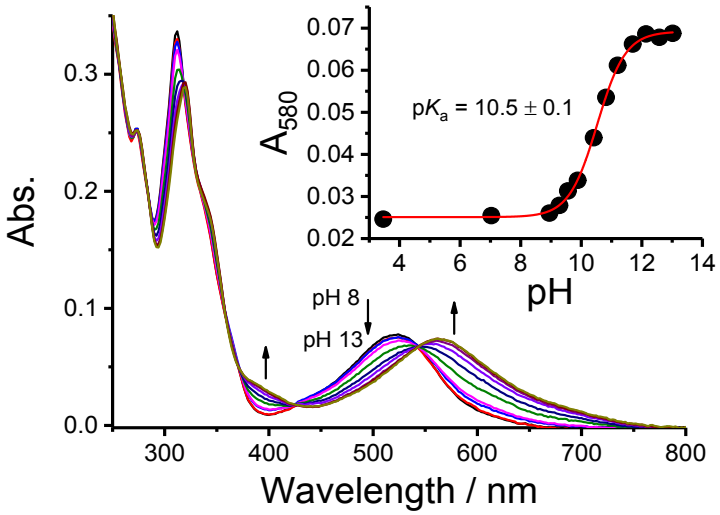

Figure S26. Absorption spectra of *distal*-**1** during pH titration experiment in an aqueous buffer containing in boric acid (0.1 M), KH_2PO_4 (0.05 M), and citric acid (0.02 M).

Additional figures for photo- and thermal-isomerization

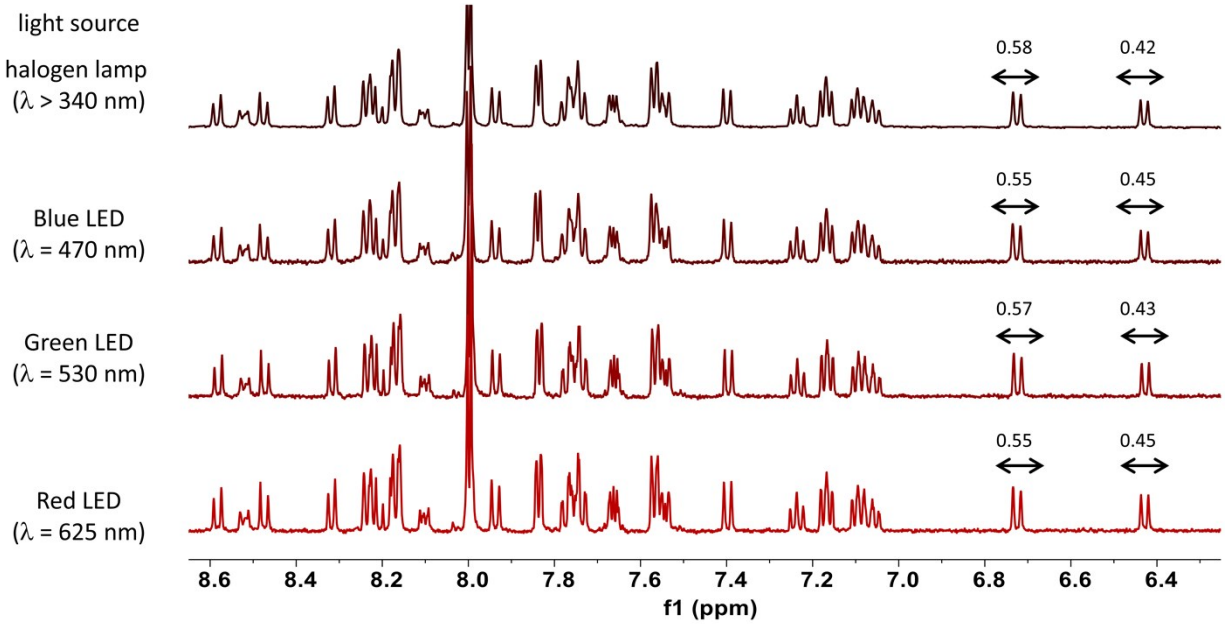

Figure S27. ^{1}H NMR spectra of *proximal*-**1** (2mM) in 20% CD_3OD and 80% D_2O after light irradiation with different light source. The samples were irradiated with light sources until they reached photostationary state. Peaks at 6.72 and 6.42 ppm correspond to *distal*-**1** and *proximal*-**1**, respectively.

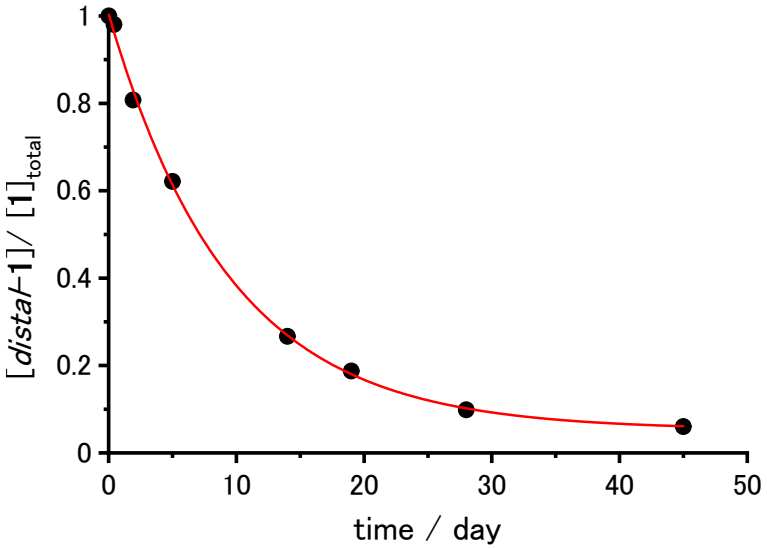

Figure S28. Kinetic traces for thermal-back-isomerization of *distal*-**1** to *proximal*-**1** at room temperature in CD_3OD (20%) and D_2O (80 %). The proportion of *distal*-**1** to the total concentration were estimated form the integration of peaks at 6.72 ppm (*distal*-**1**) and 6.42 ppm (*proximal*-**1**).

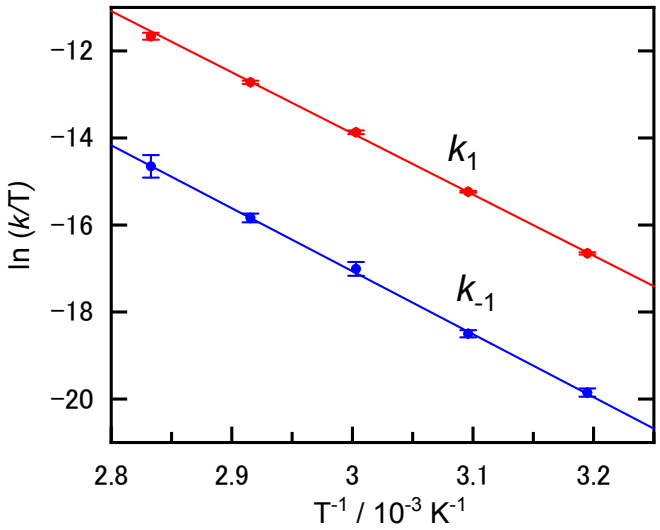

Figure S29. Eyring plots for the thermal isomerization between *proximal*-**1** and *distal*-**1**. Distal to proximal (k_1, red) and proximal to red (k_{-1}, blue).

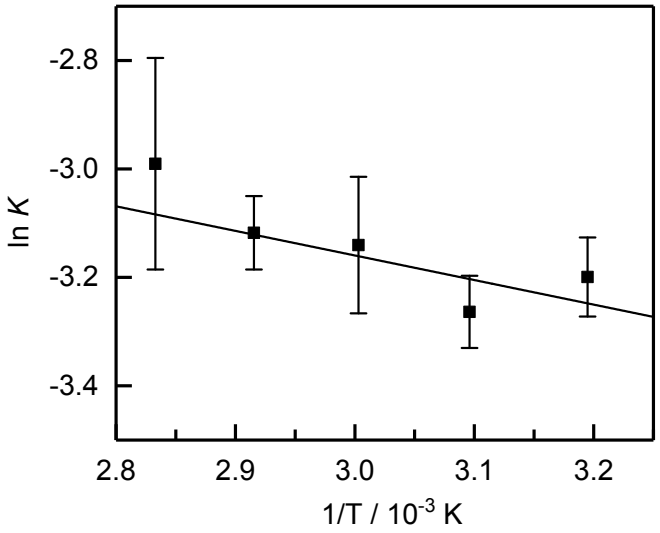

Figure S30. van't Hoff plots for the thermal isomerization between *proximal*-**1** and *distal*-**1** ,where the equilibrium constant K was defined as $K = k_{-1} / k_1$.

Table S1. Summary of photoisomerization and thermal isomerization parameters

	Photoisomerization	Thermal isomerization			
Reaction	Φ [a]	ΔG / kJ mol^{-1} [b]	ΔH‡ / kJ mol^{-1}	ΔS‡ / J K^{-1} mol^{-1}	ΔG‡/ kJ mol^{-1}
proximal-**1** → *distal*-**1**	2.7×10^{-3}	8 ± 3	117 ± 2	37 ± 1	106 ± 2
distal-**1** → *proximal*-**1**	1.9×10^{-3}	-8 ± 3	120 ± 2	22 ± 1	113 ± 2

[a]Excitation wavelength: 509 ± 1.5 nm (1.6 mW cm^{-2}). Solvent: D_2O 80% and CD_3OD 20%. [b]at 298 K

Additional Figures for catalytic oxygen evolution

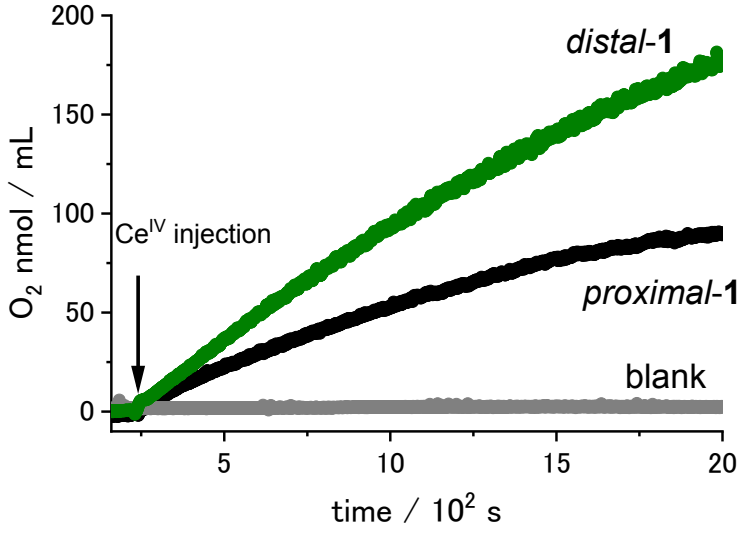

Figure S31. Catalytic oxygen evolution from *distal*-**1** (green), *proximal*-**1** (black), and blank (gray) at room temperature. Conditions: 68 μM catalyst, 0.05 M ceric ammonium nitrate in 0.1 M triflic acid. Evolved oxygen was analyzed by Clark oxygen electrode.

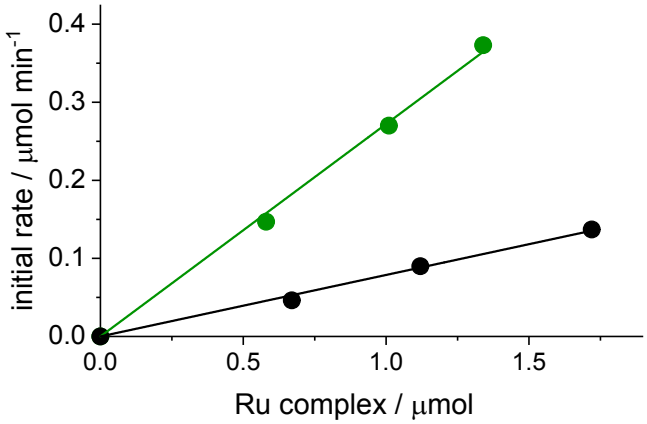

Figure S32. Plots of initial rate (v_{O2} / mol s^{-1}) of O_2 evolved vs the amount of Ru complex for *proximal*-**1** (black) and *distal*-**1** (green). Conditions: ruthenium complexes, 39-104 μM catalyst, 0.05 M ceric ammonium nitrate in 0.1 M triflic acid. Evolved oxygen was analyzed by gas chromatography.

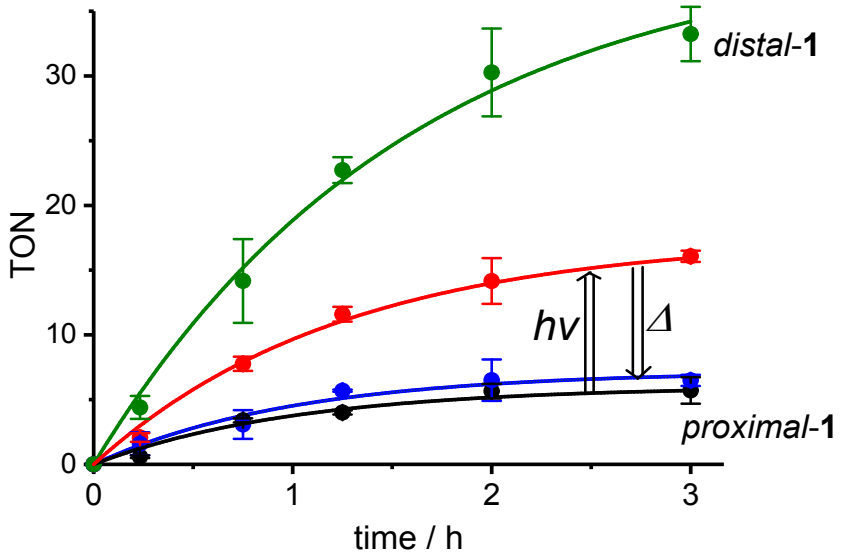

Figure S33. Catalytic oxygen evolution from $Ce^{IV}(NH_4)_2(NO_3)_6$ (0.05 M) in the presence of a ruthenium catalyst (67 μM) in 0.1 M triflic acid (15 mL) and trifluoroethanol (20 μL). *Proximal*-**1** (black), *proximal*-**1** after light irradiation at room temperature (red), *proximal*-**1** after the light irradiation followed by heating at 333 K overnight in the dark (blue), and *distal*-**1** (green). The external stimuli was applied prior to the mixing with $Ce^{IV}(NH_4)_2(NO_3)_6$.

Electrochemical measurements

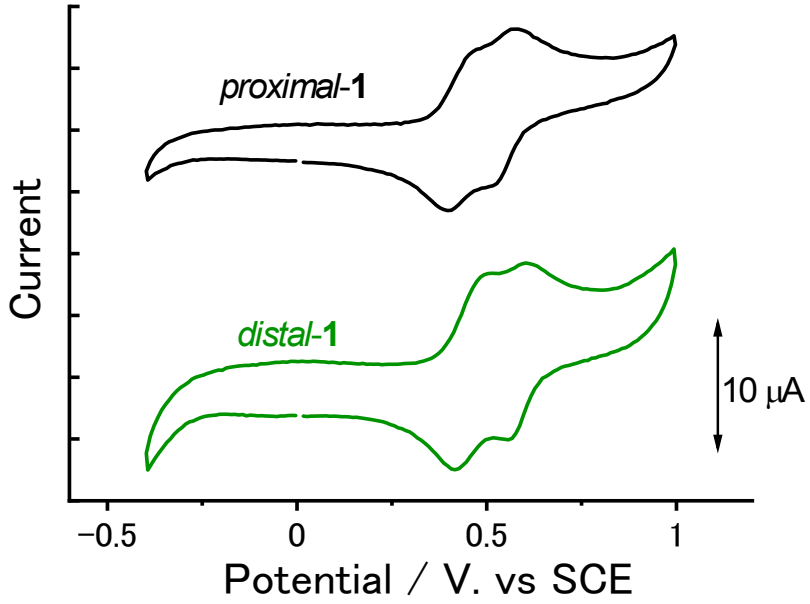

Figure S34. Cyclic voltammograms of 1 mM *proximal*-**1** (top, black) and *distal*-**1** (bottom, green) in a mixed buffer solution (5 mM $Na_2B_4O_7$, 10 mM KH_2PO_4, 5 mM citric acid, pH 7) using glassy carbon electrode (0.071 cm^2) at room temperature. (scan rate = 100 mV s^{-1}).

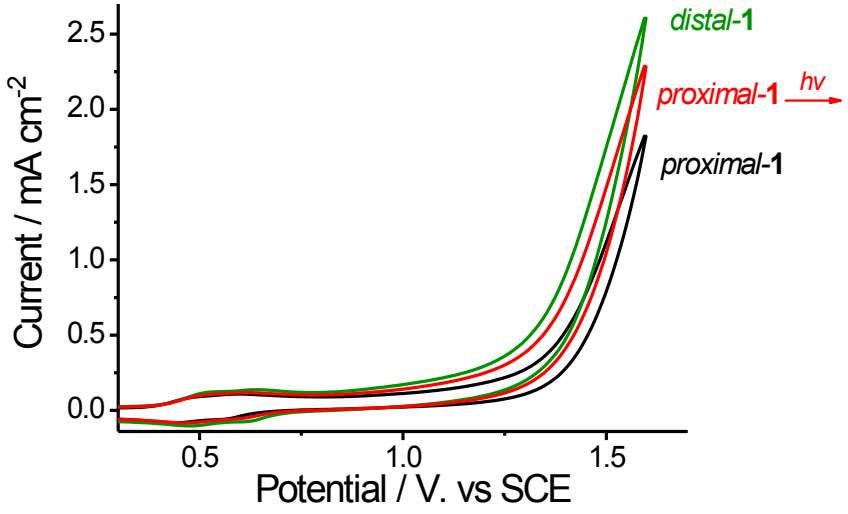

Figure 35. Cyclic voltammograms of 1 mM *proximal*-**1** (black), *proximal*-**1** after light irradiation with Xenon lamp (λ>340 nm, 70 mW cm^{-2}) for 2h (red), and *distal*-**1** (green) in a mixed buffer solution (5 mM $Na_2B_4O_7$, 10 mM KH_2PO_4, 5 mM citric acid, pH 7) using glassy carbon electrode (0.071 cm^2) at room temperature. (scan rate = 100 mV s^{-1}).

Crystallographic information

Refinement details

Table S1. Selected crystallographic parameters

compounds	*proximal*-[**1**](OTf)$_2$·2H$_2$O	*distal*-[**1**](OTf)$_2$·2H$_2$O
empirical formula	$RuO_3N_5C_{33}H_{31}$, 2(CF_3O_3 S), 2(H_2O)	$RuO_3N_5C_{33}H_{31}$, 2(CF_3O_3 S), 2(H_2O)
fw	980.9	980.9
radiation	Mo Kα	Mo Kα
crystal system	triclinic	triclinic
space group	*P*1	*P*$\bar{1}$
a, Å	10.011(4)	11.5955(2)
b, Å	13.646(5)	13.3944(2)
c, Å	16.369(6)	13.4286(2)
α, deg	66.564(5)	94.6542(9)
β, deg	72.663(5)	108.3216(8)
γ, deg	78.969(5)	99.0418(9)
V, Å^3	1951.7(12)	1936.28(5)
Z	2	2
μ, mm^{-1}	0.604	0.609
T, K	100	100
d_{cal}, g/cm^3	1.669	1.682
T_{min}, T_{max}	0.6786, 0.7456	0.704, 0.746
N_{ref}	17689	9001
$R[F^2 > 2\sigma(F^2)]$	0.0647	0.0391
$wR[F^2 > 2\sigma(F^2)]$	0.1027	0.0840
GOF	1.0033	1.051

Table 2. Selected bond distances (Å) and angles (°) for *proximal/disital*-**1**, *proximal/distal*-**2** ([Ru(tpy)(pq)OH_2]$^{2+}$), and *proximal*-**Cl** ([Ru(tpy)(6'-chloro-pyridiylquinoline)OH_2]$^{2+}$).

	proximal-**1**	*distal*-**1**	*proximal*-**2**[8]	*distal*-**2** [8]	*proximal*-**Cl**[9]
Ru1-O1	2.148(3)	2.134(2)	2.137(8)	2.132(5)	2.129(4)
Ru1-N1	2.079(4)	2.108(8)	2.061(8)	2.064(5)	2.091(4)
Ru1-N2	1.951(4)	1.966(6)	1.937(7)	1.970(5)	1.961(3)
Ru1-N3	2.057(5)	2.043(6)	2.060(8)	2.069(5)	2.070(4)
Ru1-N4	2.064(4)	2.058(3)	2.091(9)	2.067(5)	2.057(4)
Ru1-N5	2.110(4)	2.102(3)	2.139(9)	2.103(5)	2.096(3)
O1-Ru1-N1	87.21(14)	85.9(3)	86.9(3)	87.6(2)	87.51(15)
O1-Ru1-N2	81.09(15)	79.9(2)	84.0(3)	84.4(2)	84.44(14)
O1-Ru1-N3	87.63(15)	88.12(18)	91.0(3)	88.7(2)	89.52(15)
O1-Ru1-N4	177.14(17)	98.85(10)	175.5(3)	91.6(2)	170.76(14)
O1-Ru1-N5	100.64(14)	172.82(12)	105.1(3)	170.6(2)	95.33(14)
N1-Ru1-N2	79.71(18)	78.1(3)	79.7(3)	79.3(2)	79.53(15)
N1-Ru1-N3	159.35(17)	158.5(2)	159.5(3)	159.5(2)	158.81(13)
N1-Ru1-N4	90.30(16)	97.9(2)	88.6(3)	101.7(2)	87.09(16)
N1-Ru1-N5	94.23(17)	87.4(3)	101.3(3)	94.0(2)	98.12(15)
N2-Ru1-N3	79.74(18)	80.5(2)	79.9(3)	80.2(2)	79.31(15)
N2-Ru1-N4	99.86(17)	175.83(18)	94.4(3)	175.8(2)	101.93(15)
N2-Ru1-N5	173.65(17)	101.4(2)	170.8(3)	105.0(2)	177.64(17)
N3-Ru1-N4	95.19(17)	103.47(16)	92.9(3)	98.6(2)	98.20(16)
N3-Ru1-N5	106.37(17)	99.05(19)	98.9(3)	92.9(2)	103.04(14)
N4-Ru1-N5	78.13(17)	79.28(10)	76.6(4)	79.0(2)	78.03(14)
O1-Ru1-N4-O3		14.91 (12)			
O1-Ru1-N5-C31	24.6 (2)		4.5978(12)		

DFT calculations

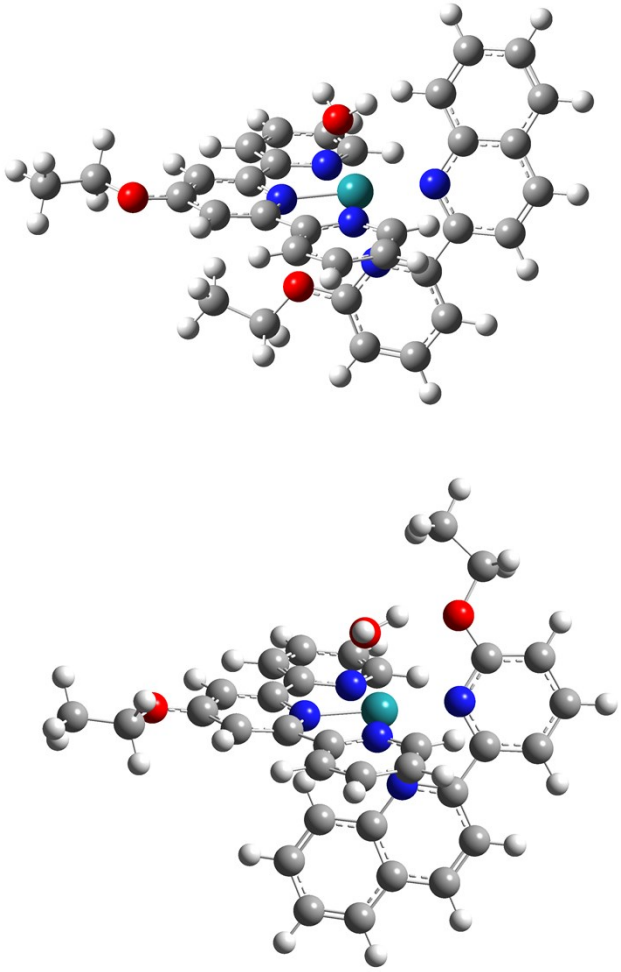

Figure S36. Optimized structures of *proximal*-**1**(top) and *distal*-**1** (bottom). The sum of electronic and thermal free energy for *proximal* and *distal*-**1** were -1868.821662 and -1868.827547 a.u., respectively. The thermal free energy of *distal*-**1** was lower than that of *proximal*-**1** by 15.45 kJ mol^{-1}.

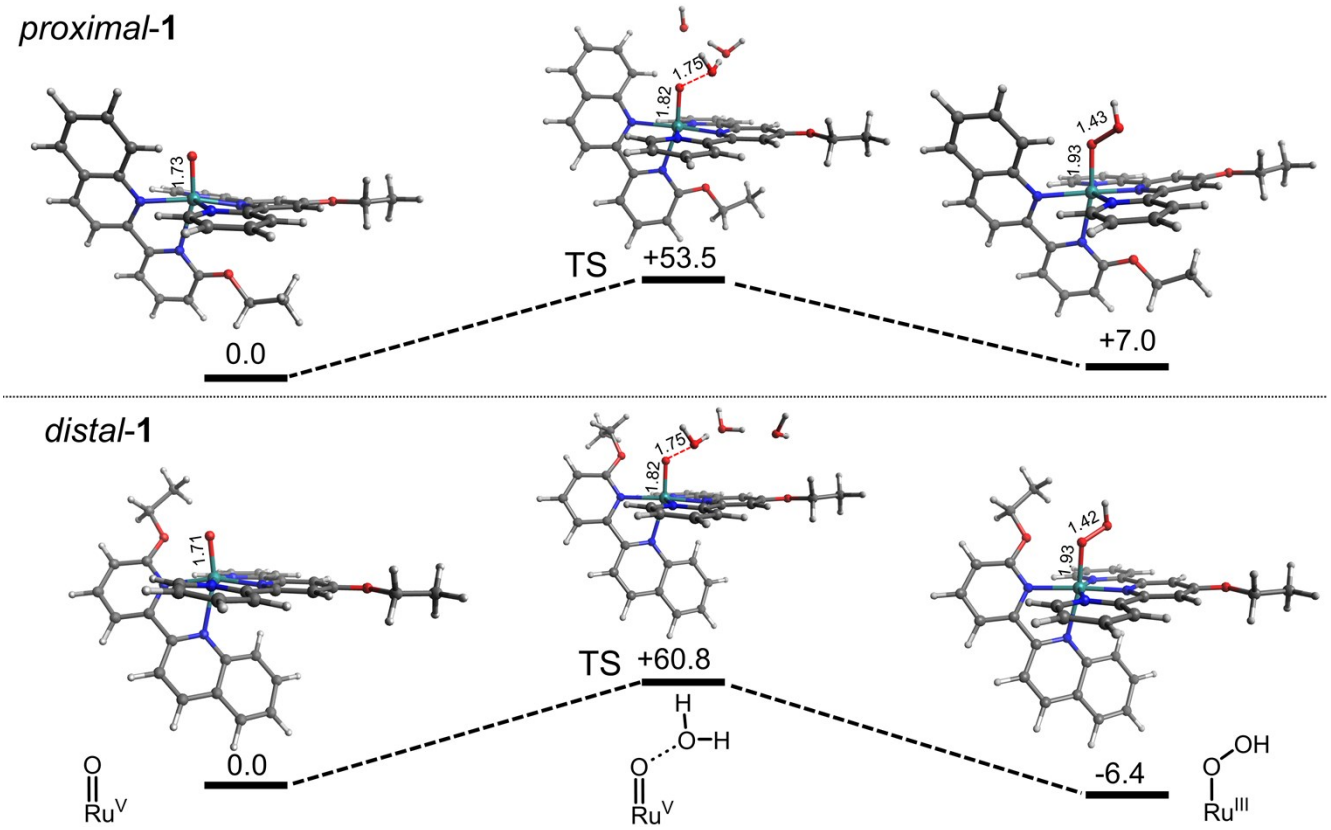

Figure S37. Energy diagram by DFT calculations for nucleophilic attack of the water molecule to the Ru^{V}=O to form peroxide spccies. The values are in kJ/mol with respect to Ru^{V}=O. Transition states (TS) were modeled with the Ru^{V}=O complex with three water molecules.

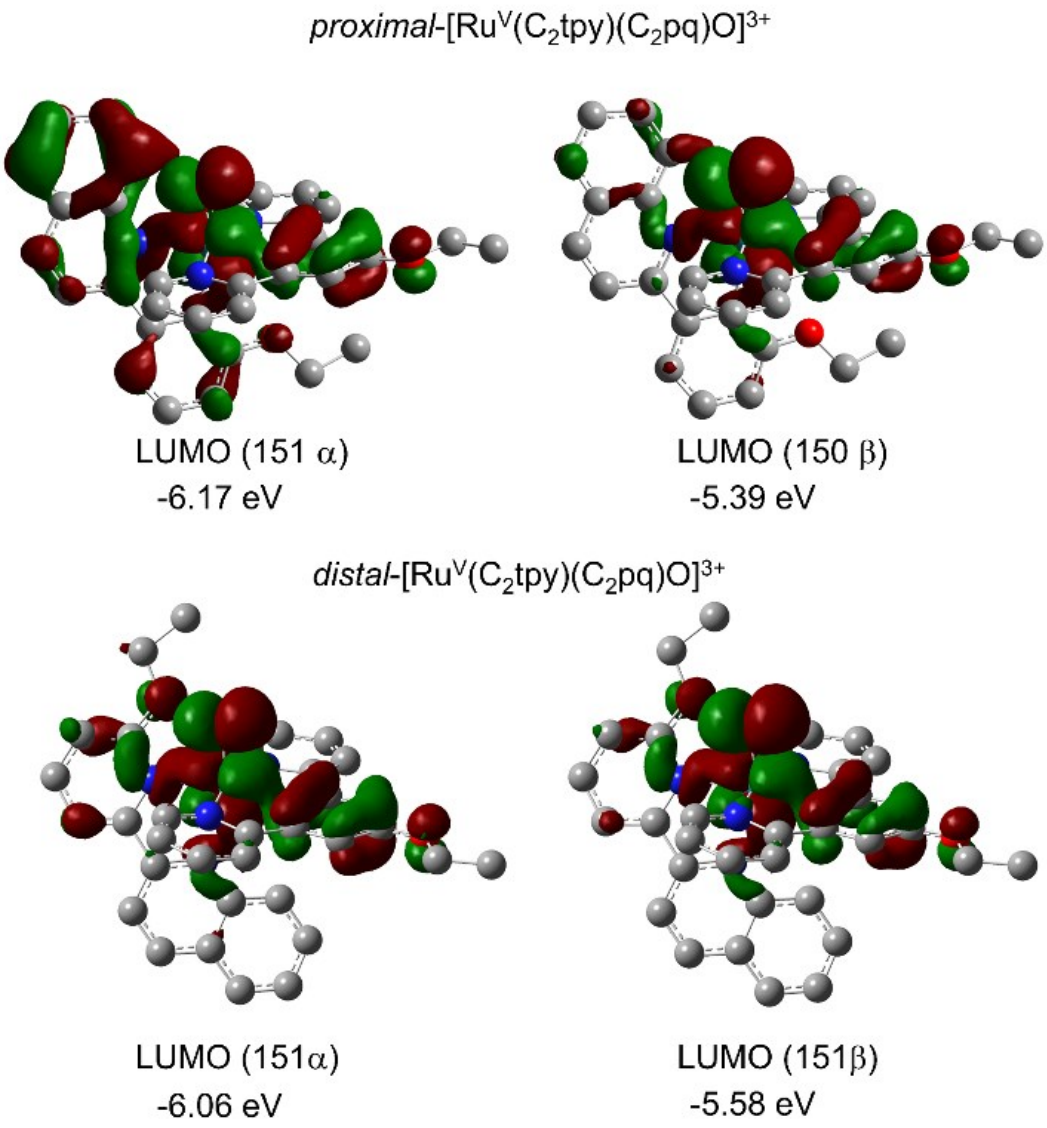

Figure S38. Lowest unoccupied molecular orbitals (LUMOs) of *proximal*- and *distal*-[Ru(C$_2$tpy)(C$_2$pq)O]$^{3+}$. Hydrogen atoms have been removed for clarity.

Cartesian Coordinates and Energies

proximal-**1** (Singlet)

Energy: -1868.821662 a.u.

Ru	-0.51525	0.14919	-0.20362
O	5.4171	-0.05091	-1.54952
O	-0.31456	1.11299	-2.20852
H	-0.02005	2.04054	-2.21762
H	-1.12641	1.08992	-2.74431
O	1.33761	-0.89872	2.24921
N	1.46971	0.02211	-0.47859
N	-2.6602	0.21531	0.01777
N	-0.36076	-1.67578	-1.3076
N	0.14932	1.90119	0.78027
N	-0.826	-0.96117	1.55515
C	1.503	2.09205	0.676
C	1.9577	-0.99473	-1.22357
C	-5.381	-0.48792	0.0337
H	-6.42352	-0.79026	0.00831
C	-0.21233	-2.28516	3.47469
H	0.55102	-2.62898	4.15751
C	0.93253	-1.98197	-1.63809
C	-1.51831	-2.72519	3.60899
H	-1.78017	-3.41861	4.40115
C	0.21315	-4.01622	-2.71468
H	0.44195	-4.92684	-3.25823
C	-1.09993	-3.69224	-2.38385
H	-1.93043	-4.3322	-2.65951
C	-4.95155	0.61333	-0.74555
C	4.13509	0.03815	-1.16579
C	-4.03869	2.87044	-2.13597
H	-3.69934	3.76734	-2.64501
C	2.37276	-1.2665	3.19833
H	2.04128	-0.98599	4.20377
H	2.51469	-2.35189	3.16143
C	-5.84482	1.38209	-1.535
H	-6.8908	1.09103	-1.56768
C	-2.12246	-1.37096	1.72159
C	-2.49157	-2.25687	2.73171
H	-3.52038	-2.56626	2.85042
C	-4.48365	-1.14061	0.83922
H	-4.81474	-1.95997	1.46252
C	2.23898	1.05676	-0.08932
C	-0.58199	2.78652	1.47785
H	-1.64501	2.58292	1.53327
C	1.35006	4.11081	1.98645
H	1.82145	4.96928	2.45304
C	-5.39704	2.4854	-2.22731
H	-6.08587	3.0741	-2.82484
C	1.23765	-3.14896	-2.33848
H	2.26616	-3.38203	-2.58686
C	2.11816	3.19441	1.26926
H	3.18858	3.3356	1.18018
C	-1.34098	-2.51368	-1.68114
H	-2.3484	-2.22383	-1.40727
C	7.69877	0.61437	-1.75929
H	8.04109	-0.33349	-1.33265
H	7.65353	0.51511	-2.8482
H	8.43014	1.39025	-1.51191
C	3.59337	1.1002	-0.42277
H	4.20638	1.93712	-0.12005
C	-0.02261	3.9024	2.09607
H	-0.65884	4.58577	2.64698
C	3.30043	-1.02096	-1.57236
H	3.72662	-1.81672	-2.16999
C	0.106	-1.38932	2.43883
C	-3.56513	0.96557	-0.70413
C	-3.14183	2.12952	-1.39405
H	-2.1167	2.45761	-1.28914
C	-3.11876	-0.75514	0.82483
C	3.64846	-0.53927	2.82874
H	3.99734	-0.83033	1.83457
H	3.50574	0.54494	2.85462
H	4.42431	-0.80116	3.55554
C	6.34455	1.00063	-1.19672
H	5.99	1.94639	-1.62291
H	6.37789	1.09594	-0.10524

distal-**1** (Singlet)

Energy: -1868.827547 a.u.

Ru	0.57904	-0.30622	0.15968
N	0.01239	0.70593	1.95643
N	-1.4208	-0.49405	0.12016
N	0.31631	-1.40172	-1.62718
C	0.80636	1.32235	2.84688
H	1.87229	1.25464	2.66293
C	0.30812	2.01246	3.94978
H	0.99472	2.49359	4.63701
C	-1.07051	2.06599	4.13797
H	-1.49661	2.59843	4.98167
C	-1.90358	1.42099	3.22466
H	-2.9786	1.45307	3.35453
C	-1.34562	0.74245	2.14153
C	-2.14946	-0.00094	1.1409
C	-3.52002	-0.24925	1.22026
H	-4.10225	0.14481	2.04079
C	-4.11639	-1.04348	0.22654
C	-3.31973	-1.5858	-0.80139
H	-3.79032	-2.22101	-1.54119
C	-1.96356	-1.29722	-0.82861
C	-0.98593	-1.77569	-1.83617
C	-1.34218	-2.54107	-2.94665
H	-2.37553	-2.82641	-3.1033
C	-0.36247	-2.93154	-3.85813
H	-0.63081	-3.52647	-4.72469
C	0.95704	-2.54187	-3.64008
H	1.75151	-2.81882	-4.32378
C	1.25281	-1.77887	-2.51309
H	2.26416	-1.45286	-2.30087
C	-6.31549	-0.8473	1.19318
H	-6.2713	0.24789	1.19028
H	-5.98795	-1.21185	2.17367
C	-7.70713	-1.34559	0.85515
H	-8.0226	-0.98157	-0.12747
H	-7.7388	-2.43947	0.85313
H	-8.41594	-0.97953	1.60462
O	-5.41858	-1.35636	0.17897
O	3.04194	-2.3652	0.77346
N	2.72058	-0.16882	0.29139
O	0.39708	-2.23722	1.19544
N	0.96809	1.60236	-0.7094
C	3.19651	1.08685	0.05764
C	2.20298	2.06532	-0.42727
C	0.37998	3.84104	-1.52789
C	-1.17794	1.98111	-1.80086
H	-1.40969	0.93388	-1.71134
C	3.5949	-1.13863	0.62784
C	1.6517	4.30794	-1.12629
H	1.90488	5.35658	-1.24909
C	2.56158	3.42345	-0.61196
H	3.54611	3.76786	-0.32772
C	0.06809	2.45645	-1.32408
C	-2.07599	2.83351	-2.40813
H	-3.018	2.43811	-2.77584
C	4.54934	1.39713	0.20663
H	4.92079	2.39308	0.01154
C	5.4335	0.39406	0.59247
H	6.48825	0.61342	0.719
C	4.96255	-0.89491	0.80034
H	5.63707	-1.68924	1.08754
C	-0.57271	4.69842	-2.13605
H	-0.316	5.74565	-2.26699
C	-1.78453	4.20812	-2.56581
H	-2.50821	4.86557	-3.03718
C	3.90284	-3.51803	1.00388
H	4.64607	-3.55395	0.20201
H	4.41141	-3.38768	1.964
H	1.33735	-2.52528	1.19337
H	0.16561	-2.10577	2.13184
C	3.02671	-4.75463	1.00108
H	2.29474	-4.72863	1.81485
H	2.50054	-4.86046	0.04746
H	3.65902	-5.63625	1.14517

proximal-$[Ru^{V}(C_2tpy)(C_2pq)O]^{3+}$ (doublet)

Energy: -1867.83890511 a.u.

Ru	-0.51707	0.17434	-0.43935
O	5.39547	-0.07805	-1.44379
O	-0.86359	0.83961	-1.99686
O	1.40656	-0.58620	2.27061
N	1.44353	0.03610	-0.55954
N	-2.63231	0.14100	0.01580
N	-0.31917	-1.78939	-1.26034
N	0.05492	1.98248	0.49938
N	-0.71810	-0.89187	1.54630
C	1.40208	2.20867	0.40786
C	1.97920	-1.08048	-1.13648
C	-5.32983	-0.52460	0.26898
H	-6.37516	-0.80658	0.34398
C	0.05973	-2.27221	3.35818
H	0.86172	-2.57442	4.01604
C	0.99046	-2.12745	-1.46460
C	-1.18260	-2.86690	3.45046
H	-1.35580	-3.65361	4.17647
C	0.31447	-4.28362	-2.28875
H	0.56657	-5.26129	-2.68446
C	-1.01379	-3.91556	-2.09712
H	-1.83091	-4.58389	-2.34096
C	-4.95922	0.56616	-0.54627
C	4.12413	0.02049	-1.11878
C	-4.17555	2.76750	-2.09238
H	-3.87631	3.64171	-2.66103
C	2.45303	-0.80471	3.27064
H	2.00206	-0.69327	4.26067
H	2.82991	-1.82487	3.15459
C	-5.91647	1.31109	-1.27857
H	-6.95768	1.00919	-1.22535
C	-1.96202	-1.43405	1.69405
C	-2.22393	-2.42927	2.62698
H	-3.20913	-2.86142	2.72796
C	-4.37521	-1.19985	0.99185
H	-4.66570	-2.00281	1.65407
C	2.18175	1.13344	-0.23738
C	-0.73538	2.86430	1.12771
H	-1.78793	2.61915	1.18838
C	1.13515	4.29733	1.57120
H	1.56172	5.20378	1.98624
C	-5.53145	2.39212	-2.04860
H	-6.27060	2.96123	-2.60191
C	1.32833	-3.37790	-1.97202
H	2.36709	-3.64627	-2.11865
C	1.96093	3.36792	0.93420
H	3.02678	3.54509	0.86267
C	-1.29304	-2.65327	-1.57737
H	-2.31152	-2.32319	-1.41705
C	7.67561	0.58739	-1.73139
H	8.02718	-0.29117	-1.18272
H	7.63557	0.35031	-2.79848
H	8.39388	1.39962	-1.58299
C	3.53431	1.15989	-0.51800
H	4.12526	2.03500	-0.28961
C	-0.22787	4.04024	1.67752
H	-0.90015	4.72823	2.17592
C	3.32612	-1.11406	-1.41701
H	3.79602	-1.96473	-1.89321
C	0.26347	-1.25637	2.39800
C	-3.57065	0.91204	-0.63768
C	-3.21011	2.05642	-1.39634
H	-2.19508	2.42355	-1.39202
C	-3.02062	-0.83268	0.86390
C	3.54728	0.21850	3.06035
H	4.03155	0.09473	2.08894
H	3.15789	1.23709	3.14607
H	4.30524	0.07605	3.83726
C	6.31999	1.03323	-1.22609
H	5.94329	1.90035	-1.77694
H	6.33620	1.25793	-0.15561

distal-[$Ru^{V}(C_2tpy)(C_2pq)O]^{3+}$ (doublet)

Energy: -1867.83607091 a.u.

Ru	-0.70714	-0.38718	-0.40200
N	-0.10605	1.13158	-1.77907
N	1.23449	-0.65853	-0.39356
N	-0.55048	-1.92856	1.04122
C	-0.88460	1.98521	-2.45648
H	-1.95311	1.90052	-2.30370
C	-0.34814	2.93613	-3.32362
H	-1.01252	3.60920	-3.85217
C	1.03221	2.99464	-3.48417
H	1.48261	3.72723	-4.14458
C	1.84198	2.09268	-2.79049
H	2.91731	2.12317	-2.91298
C	1.25192	1.15849	-1.94538
C	2.00481	0.12484	-1.20538
C	3.35669	-0.13166	-1.31872
H	3.97541	0.46936	-1.96878
C	3.90846	-1.21692	-0.59378
C	3.07144	-2.02121	0.22533
H	3.51427	-2.85359	0.75651
C	1.73405	-1.72118	0.31504
C	0.72355	-2.42385	1.13067
C	1.00956	-3.49554	1.96908
H	2.01814	-3.88359	2.03834
C	-0.01876	-4.06405	2.72414
H	0.19235	-4.90094	3.38056
C	-1.30513	-3.54273	2.62880
H	-2.12839	-3.95125	3.20250
C	-1.53640	-2.46870	1.77084
H	-2.52072	-2.03631	1.65688
C	6.14540	-0.83677	-1.44134
H	6.14575	0.20832	-1.11875
H	5.82031	-0.90018	-2.48396
C	7.49002	-1.49723	-1.22594
H	7.78863	-1.44191	-0.17518
H	7.46436	-2.54563	-1.53664
H	8.24016	-0.97503	-1.82787
O	5.17431	-1.56481	-0.62275
O	-3.55731	-1.69345	-0.71305
N	-2.71933	0.28939	-0.04393
N	-0.59377	1.35220	1.13268
C	-2.85798	1.56537	0.40939
C	-1.62723	2.18724	0.92897
C	0.63668	3.20406	2.14736
C	1.49565	0.91907	2.30653
H	1.35614	-0.14501	2.19595
C	-3.81136	-0.43376	-0.39308
C	-0.41985	4.07223	1.79609
H	-0.33419	5.13425	2.00376
C	-1.56653	3.56227	1.23541
H	-2.40026	4.21155	1.00470
C	0.50377	1.80946	1.83410
C	2.59793	1.39386	2.98702
H	3.33701	0.69010	3.35638
C	-4.10269	2.17916	0.45345
H	-4.21171	3.18789	0.82677
C	-5.22621	1.45800	0.03601
H	-6.20725	1.91937	0.06422
C	-5.09370	0.14579	-0.37867
H	-5.95756	-0.44230	-0.65664
C	1.79560	3.66425	2.82421
H	1.88649	4.72574	3.03327
C	2.76761	2.77727	3.22750
H	3.64868	3.12971	3.75344
C	-4.61140	-2.55262	-1.24869
H	-5.38165	-2.66100	-0.47944
H	-5.03697	-2.06156	-2.12830
C	-3.97126	-3.88089	-1.59196
H	-3.19472	-3.75606	-2.35200
H	-3.53197	-4.34334	-0.70315
H	-4.74045	-4.55170	-1.98708
O	-1.22104	-1.43062	-1.66032

proximal-[$Ru^{III}(C_2tpy)(C_2pq)OOH]^{2+}$ (doublet)

Energy: -1943.85076279 a.u.

Ru	-0.51271	0.16015	-0.21102
O	5.42906	0.14082	-1.43682
O	-0.59130	1.24460	-1.80582
O	1.33981	-1.21843	2.15885
N	1.47107	0.06943	-0.46460
N	-2.68214	0.14056	0.05953
N	-0.33344	-1.55202	-1.52346
N	0.11435	1.73437	1.02958
N	-0.80983	-1.23042	1.43661
C	1.46588	1.94976	0.97472
C	1.97527	-0.84880	-1.31945
C	-5.39686	-0.56455	0.07324
H	-6.44148	-0.85989	0.04945
C	-0.16753	-2.85856	3.09182
H	0.59835	-3.29695	3.71486
C	0.96825	-1.79348	-1.86657
C	-1.45875	-3.35191	3.11836
H	-1.70781	-4.18746	3.76397
C	0.29060	-3.69329	-3.18483
H	0.54012	-4.53016	-3.82842
C	-1.03163	-3.42949	-2.83956
H	-1.84815	-4.04315	-3.20208
C	-4.99852	0.64328	-0.54285
C	4.14377	0.17640	-1.07410
C	-4.15344	3.08107	-1.62072
H	-3.83637	4.04164	-2.01550
C	2.37970	-1.70611	3.05142
H	2.01718	-1.62687	4.08137
H	2.57312	-2.75888	2.82062
C	-5.93287	1.51871	-1.15349
H	-6.97935	1.22871	-1.17253
C	-2.09432	-1.69328	1.50399
C	-2.44287	-2.75873	2.32819
H	-3.45904	-3.12195	2.37727
C	-4.47035	-1.33449	0.72823
H	-4.78359	-2.23719	1.23339
C	2.22350	1.04004	0.08658
C	-0.64605	2.49985	1.82711
H	-1.70632	2.27725	1.83262
C	1.25939	3.76056	2.55079
H	1.71023	4.55065	3.14171
C	-5.51903	2.71690	-1.68871
H	-6.23589	3.39008	-2.14818
C	1.30001	-2.86508	-2.69382
H	2.33412	-3.05732	-2.95219
C	2.05500	2.96279	1.72873
H	3.12461	3.12705	1.68238
C	-1.29930	-2.34669	-2.00412
H	-2.31302	-2.10258	-1.71023
C	7.71751	0.81777	-1.50185
H	8.04848	-0.18243	-1.20610
H	7.69550	0.87425	-2.59443
H	8.44445	1.54735	-1.13134
C	3.58398	1.12562	-0.20111
H	4.18890	1.90875	0.23267
C	-0.11193	3.52505	2.60426
H	-0.76657	4.11839	3.23205
C	3.32300	-0.82384	-1.63789
H	3.76995	-1.53322	-2.32245
C	0.12795	-1.77796	2.23905
C	-3.60761	0.98947	-0.51635
C	-3.21571	2.24267	-1.05479
H	-2.18028	2.54399	-1.00791
C	-3.10793	-0.94576	0.72418
C	3.62345	-0.86680	2.85068
H	4.00727	-0.96241	1.83198
H	3.42620	0.18808	3.06280
H	4.39629	-1.21710	3.54252
C	6.35335	1.12875	-0.91827
H	6.00803	2.12559	-1.21455
H	6.36147	1.06567	0.17562
O	0.35587	2.30869	-1.90547
H	0.16979	2.62543	-2.81089

distal-[$Ru^{III}(C_2tpy)(C_2pq)OOH]^{2+}$ (doublet)

Energy: -1943.84663094 a.u.

Ru	-0.62600	-0.29503	-0.20636
N	-0.03211	0.94348	-1.88068
N	1.36420	-0.54625	-0.20075
N	-0.39406	-1.57210	1.44954
C	-0.80323	1.67330	-2.69758
H	-1.86947	1.64336	-2.50654
C	-0.27924	2.43202	-3.74300
H	-0.94523	3.00556	-4.37722
C	1.09798	2.43041	-3.94116
H	1.54504	3.01217	-4.74019
C	1.90548	1.66480	-3.09955
H	2.97869	1.65263	-3.24400
C	1.32178	0.92034	-2.07597
C	2.10147	0.05106	-1.15629
C	3.47066	-0.19137	-1.23900
H	4.06769	0.28340	-2.00380
C	4.05441	-1.07931	-0.31628
C	3.24742	-1.70809	0.65381
H	3.71105	-2.40024	1.34511
C	1.89200	-1.42502	0.68524
C	0.89987	-1.98531	1.63186
C	1.22759	-2.86604	2.66109
H	2.25348	-3.18365	2.80215
C	0.22554	-3.33373	3.51054
H	0.47105	-4.02008	4.31387
C	-1.08530	-2.90579	3.31497
H	-1.89409	-3.24273	3.95304
C	-1.35379	-2.02303	2.27163
H	-2.35584	-1.66236	2.07669
C	6.26581	-0.80321	-1.23932
H	6.23056	0.28673	-1.13305
H	5.94383	-1.07280	-2.25142
C	7.64792	-1.34592	-0.93379
H	7.95564	-1.07757	0.08145
H	7.66904	-2.43543	-1.03336
H	8.36815	-0.91910	-1.63884
O	5.35147	-1.39593	-0.28402
O	-3.34084	-2.04050	-0.62931
N	-2.75834	0.09634	-0.20548
N	-0.83293	1.61209	0.91235
C	-3.07787	1.39278	0.06222
C	-1.97707	2.23656	0.57985
C	0.02960	3.73921	1.76751
C	1.28577	1.66884	2.10238
H	1.35849	0.59581	2.02987
C	-3.74259	-0.77366	-0.51831
C	-1.14491	4.37727	1.31005
H	-1.25224	5.45181	1.42347
C	-2.15190	3.63033	0.75347
H	-3.06385	4.11048	0.42624
C	0.14863	2.32423	1.57059
C	2.26931	2.38293	2.75327
H	3.12476	1.85634	3.16505
C	-4.38197	1.86530	-0.06556
H	-4.63176	2.89201	0.16149
C	-5.38228	0.97827	-0.46562
H	-6.40373	1.32534	-0.58085
C	-5.07485	-0.35373	-0.68474
H	-5.84424	-1.06029	-0.96360
C	1.06845	4.45028	2.42202
H	0.96256	5.52378	2.54774
C	2.17447	3.78695	2.90199
H	2.96488	4.33142	3.40867
C	-4.30197	-3.07270	-0.95878
H	-5.09736	-3.07110	-0.20554
H	-4.73928	-2.84997	-1.93810
C	-3.55879	-4.39387	-0.96987
H	-2.76117	-4.38719	-1.71836
H	-3.12097	-4.60177	0.01127
H	-4.25840	-5.19913	-1.21524
O	-0.74704	-1.75337	-1.46029
O	0.07752	-2.88514	-1.21434
H	-0.09005	-3.40620	-2.02357

proximal-[$Ru^{V}(C_2tpy)(C_2pq)O]^{3+}$ TS ($3H_2O$)

(doublet)

Energy: -2097.12033371 a.u.

C	1.04589	1.38686	2.59889
C	-1.16379	1.43500	1.79715
C	-1.56353	2.20070	2.88823
C	-0.62244	2.56334	3.85310
C	0.69953	2.14822	3.71143
H	2.05864	1.03824	2.43885
H	-2.59712	2.50736	2.99112
H	-0.92595	3.15868	4.70741
H	1.45746	2.40344	4.44246
C	-2.08491	0.96042	0.73968
C	-3.42610	1.27158	0.61854
C	-4.16826	0.70681	-0.44402
H	-3.93135	1.93277	1.31087
C	-2.17777	-0.41846	-1.19065
C	-3.53353	-0.15938	-1.35637
H	-4.07977	-0.59625	-2.17946
C	-1.33600	-1.24659	-2.08384
C	-1.83390	-1.97353	-3.16198
C	0.84632	-1.95603	-2.57134
C	-0.95552	-2.70775	-3.95957
H	-2.89459	-1.97330	-3.38017
C	0.40512	-2.69583	-3.66567
H	1.89578	-1.91335	-2.30790
H	-1.33542	-3.27793	-4.80032
H	1.12224	-3.24483	-4.26437
N	0.14324	1.04703	1.66481
N	-1.50417	0.13706	-0.16546
N	0.00289	-1.25781	-1.79764
Ru	0.48657	-0.04290	-0.10655
C	5.66789	2.43026	-1.02831
C	5.97828	1.09200	-0.94612
C	4.98780	0.14505	-0.58016
C	3.64270	0.57745	-0.33273
C	4.35452	2.86361	-0.73332
H	6.29609	-1.57938	-0.62074
H	6.42886	3.15482	-1.30007
H	6.98580	0.73740	-1.14218
C	5.28906	-1.22556	-0.42234
H	4.10997	3.92053	-0.75895
C	3.00769	-1.61786	0.23905
C	4.32166	-2.09295	0.01751
H	4.56553	-3.13269	0.18216
C	3.36306	1.96560	-0.39485
N	2.66458	-0.34125	0.00008
C	1.95864	-2.49598	0.79896
C	2.21797	-3.80618	1.18351
C	-0.23066	-2.62294	1.63281
C	1.20448	-4.54169	1.79909
H	3.18715	-4.25640	1.02608
C	-0.02216	-3.95316	2.04318
H	1.38290	-5.56821	2.10079
H	-0.80641	-4.50668	2.53862
N	0.73130	-1.92518	0.98912
O	0.74759	1.40335	-1.17567
O	-0.60420	2.09817	-2.03323
H	-0.67233	3.02957	-1.43757
H	-0.09860	2.30375	-2.84569
O	1.70591	5.09197	-0.42555
H	1.90531	5.62062	-1.21653
H	1.80885	5.71040	0.31741
O	-0.74706	4.07218	-0.58465
H	0.15555	4.50846	-0.51096
H	-1.35801	4.75046	-0.92110
H	2.37825	2.33867	-0.15487
O	-1.36642	-1.95581	1.84738
C	-2.41066	-2.61124	2.62689
C	-3.53668	-1.62698	2.85719
H	-1.97539	-2.93462	3.57724
H	-2.75692	-3.48872	2.07202
H	-3.18429	-0.74157	3.39419
H	-4.30301	-2.11446	3.46847
H	-3.99808	-1.31962	1.91565
O	-5.45068	1.05200	-0.49680
C	-6.30835	0.52260	-1.54371
C	-7.69075	1.10379	-1.32646
H	-6.31355	-0.57014	-1.47075
H	-5.89618	0.81600	-2.51506
H	-8.36579	0.72386	-2.09966
H	-8.08591	0.81420	-0.34817
H	-7.66880	2.19577	-1.39126

distal-[$Ru^{V}(C_2tpy)(C_2pq)O]^{3+}$ TS ($3H_2O$)

(doublet)

Energy: -2097.11456477 a.u.

C	-1.42463	-1.66353	2.52857
C	0.85795	-1.34242	2.07534
C	1.20499	-1.99197	3.25613
C	0.19875	-2.48935	4.08603
C	-1.13435	-2.32057	3.72158
H	-2.44348	-1.50668	2.19930
H	2.24581	-2.10578	3.53251
H	0.46008	-2.99681	5.00829
H	-1.94422	-2.68633	4.34160
C	1.84411	-0.74629	1.14281
C	3.21876	-0.78041	1.26998
C	4.01525	-0.15148	0.28484
H	3.71275	-1.28900	2.08781
C	2.01150	0.52585	-0.86026
C	3.39890	0.51994	-0.79047
H	3.98980	1.00302	-1.55483
C	1.19562	1.13083	-1.93743
C	1.73039	1.87689	-2.98394
C	-0.96359	1.37808	-2.81987
C	0.88293	2.37964	-3.97190
H	2.79523	2.06804	-3.03192
C	-0.48286	2.12196	-3.89481
H	-2.01746	1.14923	-2.71946
H	1.29131	2.96205	-4.79061
H	-1.17423	2.48526	-4.64590
N	-0.45860	-1.19207	1.72613
N	1.28400	-0.09602	0.09040
N	-0.15244	0.90204	-1.86444
Ru	-0.69651	-0.25988	-0.16250
C	0.87338	4.75294	2.41888
C	-0.31073	5.07395	1.79529
C	-1.11707	4.06127	1.21537
C	-0.67811	2.69642	1.24500
C	1.27994	3.40051	2.49676
H	-2.71221	5.37434	0.56444
H	1.48574	5.52812	2.86790
H	-0.65703	6.10207	1.74947
C	-2.36525	4.34707	0.61909
H	2.19330	3.14371	3.02411
C	-2.65358	1.99728	0.18137
C	-3.14216	3.32325	0.13883
H	-4.11013	3.53355	-0.29449
C	0.52662	2.39694	1.92453
N	-1.43204	1.69860	0.65946
C	-3.48768	0.86609	-0.27267
C	-4.84547	0.99128	-0.54454
C	-3.57837	-1.45708	-0.58579
C	-5.57333	-0.15537	-0.87218
H	-5.34523	1.94738	-0.48025
C	-4.95192	-1.39133	-0.88197
O	-2.87248	-2.58052	-0.49674
H	-6.63326	-0.08133	-1.09066
H	-5.51518	-2.29027	-1.09099
N	-2.85869	-0.34029	-0.33947
O	-0.54437	-1.81824	-1.08092
O	0.87607	-2.00983	-2.08427
H	1.45055	-2.76734	-1.53931
H	0.40743	-2.45961	-2.81571
O	4.75756	-2.82807	-1.32033
H	5.37457	-3.12849	-0.63211
H	5.09474	-3.22246	-2.14227
O	2.25242	-3.61178	-0.81274
H	3.21167	-3.37856	-0.99661
H	2.13275	-4.53325	-1.10069
H	0.83595	1.36990	2.03300
C	-3.43257	-3.87034	-0.86727
C	-4.14760	-4.52471	0.30340
H	-4.47776	-5.52550	0.00548
H	-5.02705	-3.95585	0.62017
H	-3.47039	-4.62465	1.15708
H	-2.55623	-4.44751	-1.16597
H	-4.07424	-3.74799	-1.74406
O	5.32673	-0.25194	0.46010
C	6.23810	0.25227	-0.55402
C	7.64440	-0.06534	-0.08850
H	6.08300	1.33088	-0.66090
H	6.00230	-0.24746	-1.49867
H	8.36033	0.30162	-0.83060
H	7.85827	0.41921	0.86891
H	7.78176	-1.14527	0.02164

References

(1) Lowe, G.; Droz, A. S.; Vilaivan, T.; Weaver, G. W.; Tweedale, L.; Pratt, J. M.; Rock, P.; Yardley, V.; Croft, S. L. Cytotoxicity of (2,2':6',2' '-Terpyridine)platinum(II) Complexes to Leishmania donovani, Trypanosoma cruzi, and Trypanosoma brucei. *J. Med. Chem.* **1999**, *42*, 999-1006.

(2) Yagi, M.; Tajima, S.; Komi, M.; Yamazaki, H. Highly active and tunable catalysts for O_2 evolution from water based on mononuclear ruthenium (II) monoaquo complexes. *Dalton Trans.* **2011**, *40*, 3802-3804.

(3) Hirahara, M.; Tsukamoto, A.; Goto, H.; Tada, S.; Yagi, M.; Umemura, Y. Visible-Light-Induced Morphological Changes of Giant Vesicles by Photoisomerization of a Ruthenium Aqua Complex. *Chem. Eur. J.* **2016**, *22*, 2590-2594.

(4) Frisch, M. J.*et al.* Wallingford CT, 2009.

(5) Becke, A. D. Density-functional thermochemistry. III. The role of exact exchange. *J. Chem. Phys.* **1993**, *98*, 5648-5652.

(6) Lee, C.; Yang, W.; Parr, R. G. Development of the Colle-Salvetti correlation-energy formula into a functional of the electron density. *Phys. Rev. B* **1988**, *37*, 785-789.

(7) O'boyle, N. M.; Tenderholt, A. L.; Langner, K. M. cclib: A library for package-independent computational chemistry algorithms. *J. Comput. Chem.* **2008**, *29*, 839-845.

(8) Takahashi, K.; Zhang, X.; Hirahara, M.; Sato, T.; Saito, K.; Yui, T.; Yagi, M. Influence of chloro substituent on photoisomerization, redox reactions and water oxidation catalysis of mononuclear ruthenium complexes. *J. Photochem. Photobiol. A-Chem.* **2015**, *313*, 117-125.

(9) Hirahara, M.; Goto, H.; Yamamoto, R.; Yagi, M.; Umemura, Y. Photoisomerization and thermal isomerization of ruthenium aqua complexes with chloro-substituted asymmetric bidentate ligands. *RSC Advances* **2019**, *9*, 2002-2010.